



Universidade do Minho

Escola de Engenharia

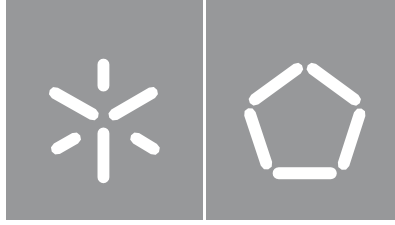
Bárbara Rodrigues Machado

Localize drug delivery systems for skin injury via alga-based electrospun nanofibers

Localize drug delivery systems for skin injury via alga-based electrospun nanofibers

UMinho | 2023 | Bárbara Machado

April 2023



Universidade do Minho

Escola de Engenharia

Bárbara Rodrigues Machado

Localize drug delivery systems for skin injury via algae-based electrospun nanofibers

Master's Dissertation

Integrated Master's Degree in Biomedical Engineering Biomaterials,
Rehabilitation and Biomechanics Branch

Project supervised by

Doctor Raúl Manuel Esteves Sousa Figueiro Doctor Diana Sara Pereira
Ferreira

COPYRIGHT AND CONDITIONS OF USE OF THE WORK BY THIRD PARTIES

This is an academic work that may be used by third parties provided that internationally accepted rules and good practices regarding copyright and related rights are respected.

Therefore, this work may be used under the terms of the license set out below.

If the user needs permission to use the work under conditions not foreseen in the license indicated, he/she should contact the author, through RepositórioUM of the University of Minho.

License granted to the users of this work



Attribution-NonCommercial-ShareAlike CC BY-NC-SA

<https://creativecommons.org/licenses/by-nc-sa/4.0/>

ACKNOWLEDGEMENTS

With the conclusion of this dissertation, I want to thank everyone who, in some way, contributed to the finalization of this stage. I would like to thank my supervisors from the University of Minho, Diana Ferreira, for her dedication to me and my project, for her guidance, kindness and for sharing her knowledge and Raúl Fanguero, director of Fibrenamics, for ensuring all the conditions for us to learn and evolve.

I would also like to show my gratitude to the whole team at Fibrenamics, which was tireless in the lab, and in particular, the PhD student Sofia Costa, for all her help, availability, dedication and care. I would also like to express my appreciation to my classmates, Margarida Pinheiro, Pedro Silva, Joana Rocha, and Gonçalo Garrett, who accompanied me in this project, supporting me every day and congratulating the achievements. Thank you for all the laughs, patience, and support.

Also, a huge thank you to my best old friends, Inês Machado, Ana Cristina and Ana Almeida for your unconditional love and patience, without you I would not have been able to overcome this goal of my life. Finally, the biggest thank you of all goes to my family, my mom, my dad, my two brothers and sister, and grandparents, for always being with me, in good and bad times and helping me to always want to be better.


To my parents, brothers and sister, and my friends, I dedicate this dissertation.

STATEMENT OF INTEGRITY

I hereby declare having conducted this academic work with integrity. I confirm that I have not used plagiarism or any form of undue use of information or falsification of results along the process leading to its elaboration.

I further declare that I have fully acknowledged the Code of Ethical Conduct of the University of Minho.

Universidade do Minho, 04/04/2023

Signature: 

Resumo

O crescimento excessivo e a acumulação de macroalgas está a tornar-se um problema grave para o ecossistema. Neste sentido, muitas estratégias têm sido estudadas de forma a controlar este crescimento e que permitam a valorização destas macroalgas, uma vez que representam um recurso natural de numerosos compostos valiosos, como o alginato e a celulose. Neste sentido, este projeto visa a produção de nanofibras por *electrospinning* baseadas em compostos extraídos de algas, nomeadamente alginato, para atuar como sistemas localizados de libertação de compostos bioativos para o tratamento de lesões da pele. Primeiramente, procedeu-se à otimização da extração de alginato de sódio (SA) da alga *Laminaria ochroleuca*. Após várias tentativas, o SA foi extraído com sucesso da alga recorrendo ao Processo 3 que consistiu numa etapa de despigmentação com etanol, uma etapa de extração, utilizando o ácido cítrico, e com carbonato de sódio, terminando com a precipitação do SA com etanol. Todo o processo foi realizado à temperatura ambiente e com tempos de reacção curtos. O rendimento de extração foi de aproximadamente 40 %, revelando-se bastante promissor em comparação com outros estudos de extração de alginato de algas recorrendo a processos verdes. Além disso, técnicas tais como ATR-FTIR (Espectroscopia de Infravermelhos de Reflexão Total Atenuada de Fourier), XRD (Difração de Raios-X) e TGA (Análise Termogravimétrica) confirmaram o sucesso da extração. Posteriormente, realizou-se um processo de extração de nanocelulose da alga *Ulva* Spp.. As amostras foram analisadas com microscopia ótica e os resultados não foram os mais promissores, pelo que será necessário otimizar este processo em trabalhos futuros. Posteriormente, foram desenvolvidas nanofibras por *electrospinning* de SA e poli(álcool vinílico) (SA/PVA) com um rácio ótimo de 50:50 e com parâmetros de *electrospinning* otimizados (24 KV, 14 cm e 0.2 ml/h) e de SA/PVA/*Ziziphus*, um extrato natural com atividade antibacteriana comprovada contra *Staphylococcus aureus*. As membranas produzidas foram analisadas por ATR-FTIR e FESEM, revelando a produção de nanofibras uniformes com diâmetros médios de 170 nm (SA/PVA) e 191 nm (SA/PVA/*Ziziphus*). Assim, com este projeto foi possível desenvolver um método alternativo, mais verde e sustentável, de extração de SA das algas, e a sua posterior utilização em nanofibras de *electrospinning* para feridas da pele, com a incorporação de um agente bioativo.

Palavras-chave: Algas, alginato, electrospinning, extração verde, nanocelulose, PVA, pensos para feridas da pele.

Abstract

Several ways have been studied to control the overgrowth and accumulation of macroalgae, since they represent a natural resource of numerous valuable compounds. Therefore, this project aims to produce nanofibers by electrospinning based on compounds extracted from algae to act as localized release systems for bioactive compounds. First, the extraction of sodium alginate (SA) from the algae *Laminaria ochroleuca* was optimized. After several attempts, the SA was successfully extracted from the alga using Process 3, which consisted of a depigmentation step using ethanol, an extraction step, with a weaker acid citric acid in one of the samples and HCL in another, and with sodium carbonate, a precipitation step with ethanol, and a washing step using ethanol and acetone. The entire process was performed without temperature and with reduced times, highlighting the sustainability of the methodology used. The extracted samples were analyzed in terms of extraction yield, approximately 40 %, which shows much higher results than other studies of alginate extraction with green processes. Furthermore, techniques including ATR-FTIR (Attenuated Total Reflectance-Fourier Transform Infrared Spectroscopy), XRD (X-Ray Diffraction) and TGA (Thermogravimetric analysis) confirmed the success of the extraction. Subsequently, an extraction process of nanocellulose from the alga *Ulva* spp. was performed. The samples were analyzed with optical microscopy and the results were not the most promising, so it will need to be optimized in future work. Subsequently, nanofibers were developed by electrospinning of sodium alginate and poly(vinyl alcohol) (SA/PVA) with an optimal ratio of 50:50 and with optimized electrospinning parameters (24 KV, 14 cm and 0.2 ml/h) and of SA/PVA/*Ziziphus*, a natural extract with proven antibacterial activity against *Staphylococcus aureus*. The results were very promising, showing diameters of 170 nm for SA/PVA nanofibers and 191 nm for SA/PVA/*Ziziphus* nanofibers, with uniform structures. Thus, with this project it was possible to develop an alternative, greener and more sustainable method of extracting SA from algae, and then using it in electrospinning nanofibers for skin wounds, with the incorporation of a bioactive agent.

KEYWORDS: Algae, alginate, electrospinning, green extraction, nanocellulose, PVA, wound dressing.

Table of contents

| | |
|--|------|
| Resumo..... | i |
| Abstract..... | ii |
| Table of contents..... | iii |
| List of figures..... | v |
| List of tables..... | vii |
| List of abbreviations and acronyms..... | viii |
| 1. INTRODUCTION..... | 1 |
| 1.1 Context and motivation..... | 2 |
| 1.2 Objective..... | 3 |
| 1.3 Dissertation structure..... | 4 |
| 2. STATE OF THE ART..... | 5 |
| 2.1 Wound dressing systems with natural based-materials..... | 6 |
| 2.2 Algae as a promising source of natural polymers..... | 10 |
| 2.2.1 Alginate..... | 11 |
| 2.2.2 Cellulose and its derivatives..... | 13 |
| 2.3 Extraction processes of natural compounds from algae..... | 14 |
| 2.3.1 Alginate Extraction..... | 15 |
| 2.3.2 Cellulose extraction..... | 17 |
| 2.4 Electrospun algae-based nanofibers for wound healing..... | 19 |
| 2.4.1 Electrospinning..... | 19 |
| 2.4.2 Alginate-based electrospun membranes as wound dressing systems..... | 22 |
| 2.4.3 Natural extracts..... | 26 |
| 3. MATERIALS AND METHODS..... | 28 |
| 3.1 Materials..... | 29 |
| 3.2 Methods..... | 30 |
| 3.2.1 Optimized process for the extraction of alginate from algae..... | 30 |
| 3.2.2 Nanocellulose extraction process..... | 32 |
| 3.2.3 Determination of the minimum inhibitory concentration (MIC) and the minimum bactericidal concentration (MBC) of the natural extract of <i>Ziziphus</i> | 33 |
| 3.2.4 Development of alginate-based electrospun nanofibers..... | 34 |
| 3.3 Characterization methods..... | 35 |
| 3.3.1 Evaluation of the viscosity of the polymeric solutions..... | 35 |
| 3.3.2 Extraction yield..... | 36 |

| | |
|--|----|
| 3.3.3 UV-visible spectroscopy..... | 36 |
| 3.3.4 Attenuated Total Reflectance - Fourier Transform Infrared Spectroscopy (ATR-FTIR) | 36 |
| 3.3.5 Optical microscopy | 37 |
| 3.3.6 X-Ray Diffraction (XRD) | 37 |
| 3.3.7 Thermogravimetric Analysis (TGA)..... | 37 |
| 3.3.8 Field Emission Scanning Electron Microscopy (FESEM) | 38 |
| 4. RESULTS AND DISCUSSION | 39 |
| 4.1 Alginate extraction from algae | 40 |
| 4.1.1 Optimization of alginate extraction process..... | 40 |
| 4.1.2 OPTIMIZED PROCESS – PROCESS 3 | 44 |
| I. Extraction Yield | 44 |
| II. ATR-FTIR analysis..... | 46 |
| III. XRD | 47 |
| IV. TGA | 48 |
| 4.2 Nanocellulose extraction | 49 |
| 4.2.1. Optical microscopy | 50 |
| 4.3 Alginate-based electrospun nanofibers | 52 |
| 4.3.1. Antibacterial activity of the natural extract..... | 52 |
| 4.3.2. Optimization of the development of alginate-based electrospun nanofibers..... | 53 |
| 4.3.3. Optical microscopy | 55 |
| 4.3.4 Solution viscosity | 57 |
| 4.3.5 FESEM | 57 |
| 4.3.6. ATR-FTIR..... | 60 |
| 5. CONCLUSIONS AND FUTURE WORK..... | 62 |
| 6. REFERENCES | 65 |

List of figures

| | |
|--|----|
| Figure 1 - Wound Healing process. Image modified from [7]. | 6 |
| Figure 2 - Types of wound dressings. | 8 |
| Figure 3 - Structure of A) Alginate Acid [42], B) Sodium Alginate [43] and C) Calcium Alginate [44]. | 12 |
| Figure 4 - Cellulose structure. Image modified from [51]. | 14 |
| Figure 5 - Electrospinning process. Image modified from [74]. | 20 |
| Figure 6 - Different techniques for drug incorporation by electrospinning. Image from [9]. | 22 |
| Figure 7 - Picture of rat wound dressing experiment at 1, 3, 8, 11 and 14 days after injury. Image modified from [89]. | 24 |
| Figure 8 - Electrospinning equipment used in this work. | 30 |
| Figure 9 - Schematic diagram of the optimized Process 3 for extraction of SA from <i>L. ochroleuca</i> algae. | 31 |
| Figure 10 - Schematic diagram of method used for the extraction of nanocellulose from <i>Ulva</i> spp. algae. | 32 |
| Figure 11 - Assembly for the extraction of nanocellulose from <i>Ulva</i> spp. algae using acid hydrolysis (H_2SO_4). | 33 |
| Figure 12 - Well plate for MIC determination after 24 h. | 34 |
| Figure 13 - Scheme of Process 1 for alginate extraction. | 41 |
| Figure 14 - Scheme of Process 2 for alginate extraction. | 42 |
| Figure 15 - Process 2 for alginate extraction from <i>L. ochroleuca</i> . A) Algae after ethanol treatment and filtrations. B) Supernatant after Na_2CO_3 addition and centrifugation. C) Filtered alginate after ethanol addition. D) Dried alginate in powder form. | 42 |
| Figure 16 - ATR-FTIR of the commercial SA and the extracted SA from <i>L. ochroleuca</i> algae using the extraction Process 2. | 43 |
| Figure 17 - ATR-FTIR of commercial SA and extracted SA using the Process 3 (with HCl and with citric acid). | 46 |
| Figure 18 - XRD pattern of commercial SA and extracted SA using Process 3 (with HCl and with citric acid). | 47 |
| Figure 19 - TGA and DTG curves of SA extracted with the Process 3 using citric acid. | 48 |

| | |
|--|----|
| Figure 20 – I) Optical microscopy images of the sample extracted from <i>Ulva</i> spp., 1 day after dialysis. A) 10x C) 50x; B) 20x and D) 20x; II) Optical microscopy images of the sample extracted from <i>Ulva</i> spp., 6 days after dialysis. A) and C) 10x; B) 20x; D) 50x..... | 50 |
| Figure 21 - Optical microscopy images of the sample extracted from <i>Ulva</i> spp. with pre-treatment, 6 days after dialysis. A) and B) 50x; C) and D) 20x..... | 51 |
| Figure 22 - Plate plates with the different concentrations of <i>Ziziphus</i> leaves extract: (A) 0.625 mg/mL, (B) 0.75 mg/mL, (C) 1.25 mg/mL and (D) 1.5 mg/mL..... | 52 |
| Figure 23 - Microscope images of electrospun SA/PVA nanofibers with different ratios with 100x magnification: A) 90:10; B) 80:20; C) 70:30; D) 60:40; E) 50:50..... | 56 |
| Figure 24 - FESEM images of A) SA/PVA and B) SA/PVA/ <i>Ziziphus</i> electrospun membranes. The FESEM images were obtained using different magnifications, from left to right: 5 000 (20 μ m); 15 000x (5 μ m); 50 000x (2 μ m)..... | 58 |
| Figure 25 - Diameter distribution histograms of nanofibers: A) SA/PVA; B) SA/PVA/ <i>Ziziphus</i> . .. | 59 |
| Figure 26 - ATR-FTIR spectra of SA/PVA and SA/PVA/ <i>Ziziphus</i> electrospun membranes. | 60 |

List of tables

| | |
|---|----|
| Table 1: Examples of SA/PVA electrospun nanofibers for wound dressing systems. | 23 |
| Table 2: Characteristics of the materials used in this work..... | 29 |
| Table 3: Optimized electrospinning parameters to produce SA/PVA and SA/PVA/Ziziphus electrospun nanofibers. | 35 |
| Table 4: Yield obtained in conventional and green alginate extraction process. | 44 |
| Table 5: Different parameters tested regarding the polymeric solutions and the electrospinning process as well as the main results observed during the process. | 54 |
| Table 6: Electrospun solutions with 4 % SA and 16 % PVA at different ratios..... | 55 |
| Table 7: Solution viscosity of the polymeric solutions. | 57 |
| Table 8: Specifications of SA/PVA/ <i>Ziziphus</i> electrospun nanofibers | 60 |

List of abbreviations and acronyms

ATR-FTIR – Attenuated Total Reflectance-Fourier Transform Infrared Spectroscopy

CNC - Cellulose nanocrystals

ECM – Extracellular matrix

FESEM - Field Emission Scanning Electron Microscopy

GH – Gatifloxacin

HCl - Hydrochloric acid

MIC - Minimum Inhibitory Concentration

MBC - Minimal Bactericidal Concentration

MFC - Minimal Fungicidal Concentration

MH – Moxifloxacin Hydrochloride

NFT - Naftifine

PLA – Polylactic acid

PLGA – Poly Lactic-co-Glycolic Acid

PEO - Polyethylene oxide

PVA - Poly(vinyl alcohol)

SA – Sodium Alginate

S. aureus - *S. aureus*

TGA - Thermogravimetric analysis

µm – micrometers

UV-VIS - Ultraviolet–Visible Spectroscopy

XRD - X-Ray Diffraction

ZnO – Zinc oxide

1. INTRODUCTION

1.1 Context and motivation

Marine macroalgae or seaweeds are a vast community of multicellular autotrophic organisms taxonomically organized into three large groups depending on the color of their thalli: Chlorophyta (green), Rhodophyta (red), and Phaeophyceae (brown). One of the current growing problems for ecosystems is the overgrowth of macroalgae since their accumulation threaten native oceanic species and resources worldwide. Thus, many strategies have been studied not only to control and/or eradicate invasive macroalgae, but also to reuse these algae waste. In fact, macroalgae represent a natural resource of numerous valuable compounds, such a high content of polysaccharides (alginate, cellulose, and others) with promising application in different areas. Moreover, their simple growth conditions, rapid proliferation rates and fewer inputs in seaweed cultivation (require no land and fertilizers, pesticides, and freshwater) makes them a reliable low-cost resource. The economic potential of seaweed is becoming increasingly important, with the seaweed industry representing over \$7.4 billion [1].

The natural compounds extracted from macroalgae have demonstrated great potential for several applications, including in biomedical field, due to their high biocompatibility and environmentally friendly properties. For instance, natural polymers are widely used for the development of wound dressing systems, because of good acceptance by biological systems, which prevents the immunological reactions often detected with synthetic polymers. For those reasons, marine macroalgae have become a very interesting bio-based source of several natural compounds to be used in biomedical applications, in line with circular economy [2]. Skin wounds represent a major healthcare problem with high morbidity and mortality rates associated. Traditional treatments have failed to address the complexity of wound healing [3]. The gauze, silk, bandages, and low-adhesion dressings may help to prevent bacterial infections but do not provide other benefits, such as diagnosis or active treatment [4]. Therefore, the exploration and development of innovative wound dressing systems with active properties, able to accelerate the wound healing process, have been the focus of several research works [3]. Bioactive wound dressings contain active compounds (e.g., antibiotics, antimicrobials, and vitamins) that will aid in wound healing [4].

Recently, electrospinning technique has acquiring increasing attention to produce fibers with controllable diameters ranging from micrometers (μm) to nanometers (nm). In fact, this technique stands out for its versatility, simplicity of use, accuracy, and for the possibility to easily tune the composition, structure and the mechanical characteristics of nanofiber-based membranes, which can be processed with several strategies to improve their biological properties [5]. Electrospun

nanofibers exhibit similar microstructure to extracellular matrix (ECM), acting as a support for cell proliferation, which favors the skin regeneration, making these structures advantageous to be used as wound dressing systems. Moreover, these nanostructures offer the advantages of increased adaptability to the wound, high loading capacity, controlled delivery of bioactive molecules, ability to allow gas exchange between the wound and surrounding environment and absorption of wound exudates. In this way, electrospun nanofibers demonstrate great potential to act as localized drug delivery systems (DDS) for wound healing applications [3].

Therefore, the combination of compounds extracted from algae with electrospinning could be a very interesting approach for the development of localized DDS for the treatment of skin injuries based on nanofibers membranes.

1.2 Objective

The aim of this project is the production of electrospun nanofibers based on compounds extracted from algae, with a green procedure, to act as fully natural localized drug delivery systems for skin treatment. Macroalgae represent a natural resource of numerous valuable compounds, such as polysaccharides (alginate, cellulose, and others), which have demonstrated great potential for several applications, including in wound dressing. Thus, in this work several processes were developed and optimized for the extraction and purification of alginate and nanocellulose from different algae, including *L. ochroleuca* and *Ulva* spp., taking into consideration the use of the most environmentally friendly methodologies possible. After optimization of the processes, a careful characterization of the extracted compounds was performed using different techniques, namely ATR-FTIR (Attenuated Total Reflectance-Fourier Transform Infrared Spectroscopy), UV-VIS (Ultraviolet-Visible spectroscopy), optical microscopy, XRD (X-Ray Diffraction) and TGA (Thermogravimetric analysis). After that, the electrospinnability of the compounds was tested, and not only the polymer formulations, considering the dissolution of the extracted compounds, but also the process parameters (applied voltage, flow rate, distance between needle and collector and needle diameter) were properly optimized for the development of nano-scale fibers with a suitable morphology. In addition, a natural extract of *Ziziphus* leaves, was added to give antibacterial properties to the electrospun membrane in order to better suit the application under consideration. Both developed electrospun membranes (with and without the natural extract) were characterized by optical microscopy, ATR-FTIR and FESEM (Field Emission Scanning Electron Microscopy). The

ultimate goal of this work was to obtain biopolymeric nanofibers with active properties composed of alginate extracted from seaweeds and a natural extract, with therapeutic properties for the localized treatment of skin wounds.

1.3 Dissertation structure

This document is structured in 5 sections: Section 1 includes a brief introduction to the subject under study. Section 2 covers the theoretical basis concerning to natural algae-based compounds, extraction processes of different compounds from algae, considering the greener and most sustainable ones; types of wound dressings and the wound healing process, electrospinning technique and the electrospun membranes already developed for wound dressing applications. Section 3 includes all materials and methods used in the development of this dissertation, like the extraction methods and the conditions used for the preparation of polymeric formulations as well as the parameters used in electrospinning process. Section 4 presents the set of results and discussion. Finally, Section 5 illustrates the main conclusions of the developed work as well as proposals for future work.

2. STATE OF THE ART

2.1 Wound dressing systems with natural based-materials

Over the past decades, wound care has progressively become a major worldwide public health concern, since the inefficient and defective treatment of skin damages can be fatal in some cases [5]. Every year, several million people are affected by skin injuries of an acute or chronic nature. It is estimated that 300,000 people die each year in lower middle-income countries from chronic wounds and burns worldwide. These injuries, and subsequent bacterial infections, are some of the most serious forms of trauma and require careful and effective wound management [6].

Wound healing is a complex process that involves hemostasis, angiogenesis and the eventual restoration of the skin barrier function [5]. Figure 1 illustrates the wound healing process.

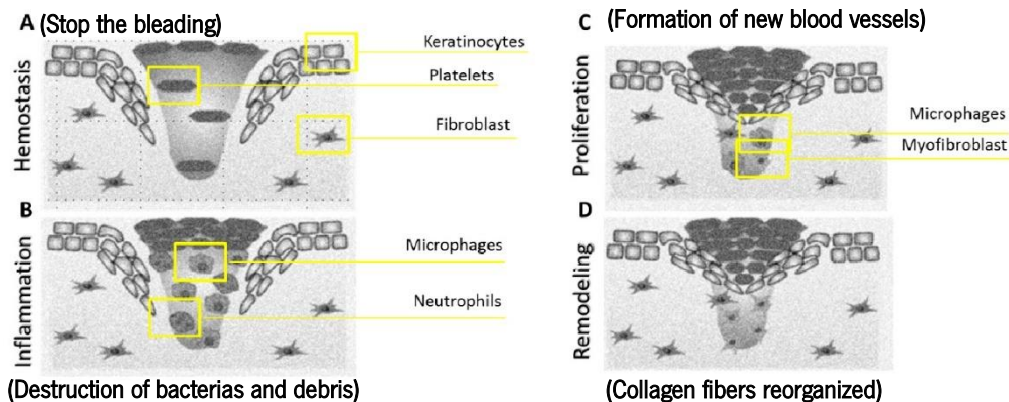


Figure 1 - Wound Healing process. Image modified from [7].

Wound healing involves several cellular and biochemical processes, starting with inflammatory reactions (immune response to prevent infection), proliferation (regeneration of tissues), and tissue remodeling [8]. The inflammatory phase follows the damaging event and includes the coagulation cascade, the inflammatory pathway, and the immune system, all to prevent excessive loss of blood, fluids, and the development of infection. Hemostasis is achieved by the generation of platelet clots, followed by the formation of fibrin matrix, which acts as a scaffold for cellular infiltration. Subsequently, the neutrophils are recruited to the lesion. New tissue formation begins, which consists of cell proliferation and migration of different cytotypes. This is followed by regeneration of the basal layer, restoring the physiological characteristics of the tissue, leaving a region rich in collagen and other extracellular matrix (ECM) deposition proteins. Acute wounds (traumatic and surgical) go through the normal stages of wound healing. Chronic wounds, on the other hand, have a persistent inflammation phase, resulting in recruitment of microorganisms and biofilm

development. Wound exudate, which represents the microenvironment of the insulted tissue, is a marker of the chronic state of an injury or a sign of the effectiveness of wound treatment [7].

In fact, the healing process is often compromised by the growth of microorganisms and the formation of biofilm on the wound surface [9], [10]. Therefore, wound dressings should contain antimicrobial agents in order to prevent or treat infections [9]. Different therapeutics are required at each phase, and the ability to administer drugs specific to each phase is crucial to enhance proper wound healing. An ideal wound dressing should have: (i) biocompatibility: cannot be toxic to the wound tissues; (ii) high absorption capacity: the excess exudates from the wound must be absorbed, otherwise it can increase the risk of bacterial growth; (iii) sufficient water vapor transmission rate: in order to decrease the risk of maceration and infection; (iv) good barrier against the penetration of microorganisms; (v) antimicrobial activity to suppress microbial growth beneath the dressing and (vi) non-adherence: adhesiveness increases the risk of repeated injury upon removal [5], [11].

Wound dressings can be classified into traditional/passive, interactive, skin substitutes, and bioactive dressings. Traditional dressings, such as wool, plaster, gauze, and bandage dressings keep the lesion protected from foreign substances or contamination, stop bleeding, cushion the lesion, and absorb wound exudate. However, they have drawbacks such as leakage of wound exudate resulting in bacterial infections and skin damage during removal [12], [13].

Interactive dressings such as composites, films, gels, foams, sprays [11], [13] have the ability to accelerate wound healing by providing a moist environment, exhibiting good water transmission, and enhancing re-epithelialization and granulation. Skin substitutes, such as Apligraf, OrCel, and TransCyte, are tissue-engineered structures, typically resulting from cell co-culture or cell-seeded scaffolding materials. However, they can cause wound infections, transmit disease, can be rejected by the body, are expensive, and have a limited lifespan.

A type of skin substitutes, are the dermal grafts, such as acellular xenografts, autografts, and allografts, which are used in traumatic wounds, burn reconstruction, defects after cancer resection, vitiligo, scar release, hair restoration, congenital skin deficiencies and the cost efficiency of its application is not yet certain [14],[12]. However, they are not suitable for managing complex injuries (i.e. conditions with exposed bone and deep spaces) [11],[14].

As mentioned above, typically, chronic wounds are susceptible to microorganisms, that cause infections and hinder the healing process. Adhesion of bacteria to a wound surface leads to the formation of biofilm. As a result, endotoxins are released, which may cause sepsis, and eventually

death. Thus, wounds should be treated with active wound dressings, containing bioactive agents, in order to prevent bacterial infection and biofilm formation in the wound environment and at the same time, promote the healing process [14]. Therefore, in recent years, an effort has been made to design new modern dressings, not only for covering, but also to protect the wound from dehydration and infections, facilitating the healing process, which are called bioactive wound dressing materials [15]. Bioactive wound dressings are a large class of wound dressing materials, including all biomaterials capable of actively stimulating wound healing, either through drug delivery mechanisms or thanks to the natural properties of the polymers used for their synthesis [16]. Hence, bioactive dressings offer considerable advantages like the interaction with the injured microenvironment, the local stimulation of cellular activity, and the inhibition of microorganism growth, which is fundamental in the perspective of faster and total recovery of tissue architecture and functionality [17]. Thus, the bioactive wound-dressings, like drug-loaded nanofiber, should act by removing the biofilm pathogenic bacteria and modulating the inflammation [18],[19]. Bioactive dressings are hydrocolloids, sponges, wafers, foams, nanofibers, hydrogels, films and they are all biodegradable, biocompatible, and can act as drug delivery systems (DDS) for therapeutic agents such as nanoparticles, grow factors (GFs), vitamins, antibiotics, which can contribute to enhance the healing process [12]. Figure 2 shows the different types of wound dressings, describing their advantages and disadvantages.

| | Traditional/passive | Interactive materials | Skin Substitutes | Dermal Graft | Bioactive dressings |
|---------------|--|---|--|---|---|
| Advantages | <ul style="list-style-type: none"> -Stop bleeding -Cushion the lesion -Absorb wound exudate | <ul style="list-style-type: none"> -Accelerate wound healing -Good water transmission -Enhancing re-epithelialization and granulation -Loaded with bioactive agents | <ul style="list-style-type: none"> -Effective in skin regeneration | <ul style="list-style-type: none"> -Use in traumatic wound, burns, defect after oncologic reception... | <ul style="list-style-type: none"> -Biodegradable -Biocompatible -Act as drug delivery systems |
| Disadvantages | <ul style="list-style-type: none"> -Bacterial infections -Damage to the skin | <ul style="list-style-type: none"> -Bacterial infections -Damage to the skin | <ul style="list-style-type: none"> -Wound infections -Transmit disease - Rejection -Expensive -Limited lifespan | <ul style="list-style-type: none"> -Not suitable for complex injuries | <p style="text-align: center;">↓</p> <p style="text-align: center;">Electrospun bioactive dressings</p> |

Figure 2 - Types of wound dressings.

Although all these examples of bioactive dressings help in wound resolution, most of them are not able to mimic the architecture of the skin and to provide a natural environment, where the cross-link between the epidermis and dermis is essential for complete tissue regeneration [20]. For these reasons, attention is slowly shifting to nanofibers produced by electrospinning to act as a wound dressing. The nanofibers' structure brings considerable advantages for this application, including the ability to mimic the extracellular matrix (ECM) architecture, which has a pivotal role in sustaining the processes of cell adhesion and proliferation, provide a high contact surface for gas exchange and fluid adsorption, easily incorporate biomolecules of interest as well as allows the possibility to adjust the composition in order to provide a physiological microenvironment for a complete wound recovery [8], [20], [21].

Natural polymers have been studied for various applications, such as the development of tissue-engineering structures and technologies of regenerative medicine, including the design of wound dressing materials. Moreover, considering the environmental concerns, the use of greener and more sustainable materials is strongly encouraged. In fact, many of these polymers have been showing a high wound healing efficiency due to the key biological properties such as antioxidant, immunomodulatory, antiviral/antibacterial, anti-inflammatory, and anticoagulant properties [22]. A wide range of natural biopolymers (e.g., alginate [23], cellulose [24], chitosan [25], gelatin [26], hyaluronic acid [27] and collagen [28]) have been explored to produce nanofibers by electrospinning for wound healing applications [18]. They own superior features including: biocompatibility, biodegradability, bioactivity, hydrophilicity and ability to interact with cells, make them particularly useful as matrices for tissue regeneration. In addition, many of them are part of the ECM composition, which helps in the similarity to the ECM and favors the wound microenvironment [20]. Other type of polymers, synthetic ones (polyethylene oxide (PEO), poly(lactic-co-glycolic acid (PLGA), poly(vinyl alcohol) (PVA), polycaprolactone (PCL), among others), possess mechanical strength and good degradation profile, which make them a favorable basis for the preparation of a wide range of medical devices, including electrospun membranes and scaffolds [20]. However, they have disadvantages such as inadequate hydrophilicity, so the mixing of natural polymers with these synthetic ones could improve the mechanical properties of natural ones, which can be advantageous for several applications [31]. Among all sources of these natural polymers, marine algae have been widely explored due to their advantages, which will be discussed in the next section.

2.2 Algae as a promising source of natural polymers

Marine algae are among the most ancient inhabitants of the planet. Several seaweeds, normally the non-natives ones, can become invasive due to their high reproductive rates, production of toxic metabolites, and their life time, which makes them more competitive than native species. Outbreaks of some invasive algae species have led to a significant negative impact on the landscape and pose a serious danger to the aquatic ecosystem [29], by causing red tides, clogging nets, clogging waterways, and altering nutrient regimes in areas near fisheries, aquaculture systems, and desalination plants [30]. Plastic pollution from landfills and rivers wreaks havoc on marine life as it causes entanglement and absorption into organs and tissues, causing toxic effects. In addition, climate change has led to increased ocean temperatures, causing greater stress on coral reefs, which leads to coral death. Nutrient-rich runoff such as sewage and agricultural discharges fuel explosive growth of harmful algae; the resulting bloom causes dead zones in the oceans and the accumulation of toxins in the ocean food chain. Therefore, recycling and valorization of these invasive algae becomes essential for both environmental and economic benefits [18], [30], [32].

Algae are photosynthetic organisms with complex and peculiar taxonomy. Currently, two main types of algae are distinguished: microalgae, consisting of a single eukaryotic cell, are widely represented in marine ecosystems as phytoplankton [29],[33], and macroalgae, having large sizes, are a multicellular heterogeneous group (red, green, and brown algae), inhabiting the littoral zone to a depth with sufficient light to drive photosynthesis [29],[34]. Over millions of years of existence in the marine ecosystem, these organisms have acquired the ability to develop effective antibiotic protection mechanisms against pathogenic microorganisms and numerous strategies for survival in extreme abiotic environmental conditions. For these reasons, many of these organisms have a unique chemical structure that others do not possess [35]. Their proliferation can offer new opportunities, as the recovery of algal biomass can contribute to various economic sectors. One of several possible applications is to obtain natural compounds with biological properties of interest to both food and pharmaceutical industries. In this way, the negative impact on ecosystems from invasive algae is stopped and a natural source that supposedly has no longer any function becomes a resource of several natural materials [31].

The dry matter of seaweeds comprises total lipids (0.5–3.5 %), proteins (3–50 %), polysaccharides (21–61 %), and minerals (12–46 %). Thus, polysaccharides are the main components of seaweed, being the amount and type dependent on the species, age or season of

harvesting, among other factors. For example, green algae contain mostly ulvan, brown seaweeds are rich in alginate, laminarin, fucans and fucoidans, while red macroalgae are composed of carrageenan, agar, floridan, starch, but also other galactans [36]. Therefore, algae waste is actually presented as a very valuable biomass resource due to its rich proteins and polysaccharides contents [29], [37]. As an example, the global phycocolloids (derived from seaweeds, like alginates, agars, and carrageenans) industries consume 594,220 dry tons of seaweed biomass annually to produce carrageenan, agar, and alginate, and what's left, residual biomass, is treated as waste or without considering for any commercial use. Currently, many works are being developed in order to convert the algae waste biomass in a high value-added products both in academia and industry fields, focusing on macroalgae as natural sources of added-value compounds [29], [37].

Biopolymers extracted from macroalgae are excellent candidates as safe biomaterials for the development of several systems for biomedical applications, namely, wound dressing systems due to their low immunogenicity bioavailability, biocompatibility, biodegradability, non-toxicity, and lack of side effects during the process of wound healing.

As mentioned earlier, macroalgae are an abundant source of polysaccharides, which are present in cell walls or vacuoles within cells. Most of these polysaccharides, mainly alginate, agar, carrageenan, fucoidan, cellulose and others have shown promising biological and physicochemical properties of relevance to biomedical applications [38]. Besides, other important and valuable components, such as pigments, vitamins and antioxidants are present in algae and can be important co-products of algae processing [39]. Carrageenans are a linear polysaccharide chains with sulfate half-esters attached to the sugar unit. They have antitumor, antiviral, anticoagulant, and immunomodulant properties that are important for wound healing and for various biomedical applications. For example, Carraguard is a carrageenan-based vaginal microbiocide that entered the clinical phase III trial conducted by the Population Council Centre in South Africa and Botswana in 2012. Thus, and because of its many advantages related to biomedical applications, namely wound dressing, alginate will be further explored below. In the following sections, two of the main components of algae, alginate and cellulose, will be discussed in more detail.

2.2.1 Alginate

Among all polysaccharides derived from algae, alginate is by far the most commonly biomaterial among other bioproducts with wound healing properties. Because of its hydrophilic nature, alginate, is capable to take multiple forms, (beads, blends, dressings, electrospun scaffolds,

flexible fibers, films, foams, gels, hydrogels, injections, microparticles, microspheres, nanoparticles, polyelectrolyte complexes, powders, ropes, sheets, sponges) that could be applied on post-traumatic wounds or exuding wounds dressing [19]. Alginates, including alginic acid and its respective salts, are a group of linear anionic polysaccharides derived from some brown algae's species. They are naturally developed in the cell wall of algae and in the bacterial capsule of *Azotobacter* spp. and *Pseudomonas* spp.. In brown algae, the alginate provides flexibility and strong structure to the algae's cell walls and protect them from possible injury when they are exposed to strong sea water waves [40]. Alginates are composed by 1,4-linked β -D-mannuronic acid (M) and α -L-guluronic acid (G) residues, that form blocks of repeated G residues, repeated M residues and alternating G and M residues in all three configurations (Figure 1) [25]. The physical and chemical properties of these linear acidic polysaccharides depend on the structural ratio of the two types of uronic acids, G and M, located in the biomolecule in the form of homo- or heteropolymer blocks [39]. Alginates with a low M/G ratio form rigid gels, contrary the ones with a high M/G ratio, which forms elastic gels [41]. The proportion and sequence of M/G units depends on the seaweed species and the location and season of collection [41].

These polysaccharides are an indispensable component of various products manufactured in the pharmaceutical and medical industry. The unique characteristics of these metabolites have found application as a therapeutic basis for nanocomposite wound dressings. Furthermore, the application of alginate in wound dressings has shown to provide a high hemostatic activity, optimum moist environment in the wound and good absorption of wound exudate, stimulate the growth of granulation tissue, reduce the concentration of pro-inflammatory cytokines, inhibit the formation of free radicals, and a pronounced [39]. Sodium alginate-based nanofibers, in addition to all these advantages, can also emulate the ECM, enhancing the epithelial cell proliferation and new tissue formation. [22].

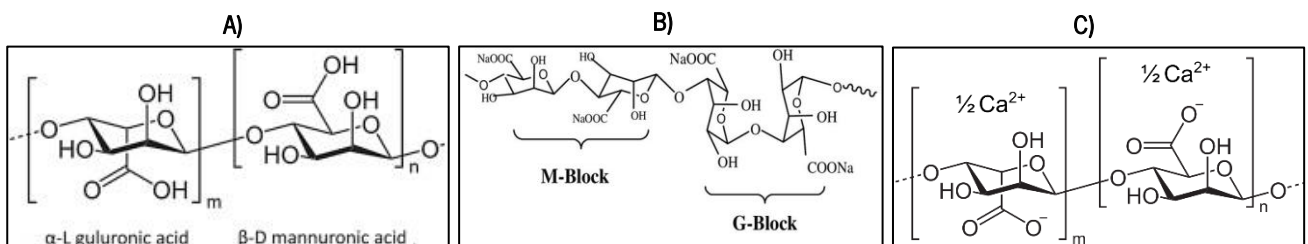


Figure 3 - Structure of **A)** Alginic Acid [42], **B)** Sodium Alginate [43] and **C)** Calcium Alginate [44].

2.2.2 Cellulose and its derivatives

Cellulose is other polysaccharide that can be extracted from algae with a high potential for biomedical applications. In particular, nanocellulose has excellent potential for wound healing applications, based on its moisture absorption and water retention capacity that can be implemented on the wound itself to help decrease inflammatory responses and promote fibroblast proliferation [45].

Cellulose is another natural, biocompatible, biodegradable, and environmentally friendly biopolymer, which plays an important role in various biomedical applications [18]. Cellulose is the major component of biomass wastes and the efficient utilization of this polymer in a high value-added products is essential. It is made up of long single chains, each of which is composed of β -d-glucopyranosyl units linked by β -1,4-glycosidic bonds. In a cellulose glucose unit, one primary (C6) and two secondary (C2, C3) hydroxyl groups are found (Figure 4) [37],[46].

There are several derivatives that can be obtained from cellulose, namely nanocellulose, which is referred to cellulosic material with one dimension in the nanometer range [47]. As an abundant and biobased material, nanocellulose can be extracted from various plant biomass, bacteria, algae using different methods, as many research studies show [48],[37]. Nanocellulose share the inherent chemical structure of cellulose with abundant hydroxyl groups and a certain amount of aldehyde groups and carboxyl groups for further functionalization. Owing to its nanostructure, nanocellulose shows significant high specific surface area, active functionalization groups, mechanical strength, crystallinity, non-toxicity and biodegradability, which makes nanocellulose a novel nanomaterial for a broad range of applications [37]. Nanocellulose mainly includes three subcategories: (i) cellulose nanocrystals (CNC), (ii) cellulose nanofibers (CNF/NFC), (iii) bacterial cellulose (BC), also defined as bacterial nanocellulose (BNC). These three types of cellulose are extracted differently. The CNC is obtained chemically, where the amorphous part is eliminated and only the crystalline part remains; the CNF is obtained mechanically, where both the amorphous and crystalline parts exist; and the BNC is produced directly by bacteria. The difference between CNF and CNC consists mainly in the dimensions and crystalline structure. CNC generally have [49] needle like-shape and present higher crystallinity and relatively smaller sizes (2–15 nm wide, 100–500 nm long), while CNF refer to nanofibrils with long lengths (20–50 nm wide, 500–1500 nm long) [26][8]. On the other hand, BNC, refers to nanostructured cellulose produced by bacteria [50]. Among all cellulose derivatives, CNC and CNF, have been widely used as a reinforcing material. For instance, it was reported that the incorporation of CNC into chitosan-based

electrospun nanofibers improved the nanofibers' morphology and diameters as well as enhanced the mechanical and thermal properties of the membranes [3].

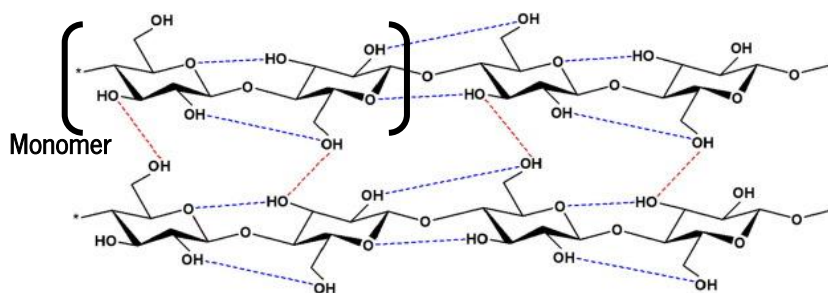


Figure 4 - Cellulose structure. Image modified from [51].

Therefore, it can be concluded that algae represent a promising source of several valuable components, such as alginate, cellulose, and other bioactive compounds that are beneficial for wound treatment. Furthermore, the use of algae waste contributes to a circular economy concept, since this waste, which may eventually prove to be harmful to the ecosystem, will be used to develop new technologies for biomedical applications. Therefore, the next section will explore the extraction methods of alginate and nanocellulose from algae, considering the most sustainable processes.

2.3 Extraction processes of natural compounds from algae

There are several published papers reporting different processes for extracting compounds from different algae. Conventional extractions pose a pollution problem because of the effluents they produce and the organic solvents that they use are not environmentally friendly [52],[53]. Besides, conventional extraction techniques are time-consuming methods and involves high energy consumption, which results in additional costs. In response to these problems, the use of "green" technology and environmentally friendly extraction methods are proposed as the key to the future [52]. More advanced extraction techniques are currently available to overcome these concerns, such as microwave-assisted extraction, accelerated solvent extraction, and ultrasound-assisted extraction (UAE). Since the extraction can be performed at a moderate temperature with a lower investment of the extraction instrument, UAE is more attractive to recover compounds from algae [53].

2.3.1 Alginate Extraction

The extraction of alginate from seaweed is always multi-stage process. The process may vary, but the steps required are the same. Firstly, the fresh algae must be treated, i.e. washed, dried and ground into a powder. Then follows the depigmentation stage, to which various chemicals can be added to remove unwanted compounds in the algae. Then an acid or alkaline pretreatment is applied to break down the cell wall, which is followed by the extraction, normally with sodium carbonate (Na_2CO_3), to obtain water-soluble alginate from the seaweed biomass matrix. There are three precipitation routes to recover alginate from solution, namely the sodium alginate (SA) route, the calcium alginate route, and the alginic acid route. To obtain SA in particular, ethanol is usually used, which reduces the solubility of the alginate and thus precipitate the SA. The fiber as the solid form of SA is then separated from the solution by filtration or centrifugation. In addition to ethanol, other organic solvents such as isopropanol and acetone can be used.

In the calcium alginate route, calcium chloride (CaCl_2) is added to the SA solution, converting the SA to insoluble calcium alginate, which can then be separated from the solution. Alginic acid also has a low solubility in water. The conversion of SA to alginic acid by the addition of hydrochloric acid (HCl) could also precipitate the alginate. In the calcium alginate and alginic acid routes, the separated solid form of alginate is commonly converted to SA by the addition of Na_2CO_3 , and subsequent precipitation using an organic solvent [54].

Conventional methods of alginate extraction use most of the times, formaldehyde and HCl, with high temperatures, in order to remove non-targeted compounds, such as polyphenols and easily degradable polysaccharides (e.g., fucoidans) and eliminate polyvalent cations, such as Ca^{2+} and Mg^{2+} by converting alginate from the salt form into alginic acid [55], [56]. However, both (HCl and formaldehyde) are considered toxic chemicals and because of that the effluents and residues of alginate extraction must be treated and recycled appropriately to limit the environmental impact [57]. The need for high temperatures and times is desirable to extract a higher yield of alginate, but poses disadvantages, such as non-preservation of the molecular weight of the alginate. Thus, the need to develop more environmentally friendly, more efficient extraction processes as well as to minimize the use of harmful chemicals is a demand for future industries. So, it is recommended to reduce the extraction temperature, usually to room temperature values (25°C), and the extraction time to a few hours [58].

Some of the alternatives mentioned may involve the replacement of toxic solvents with weaker ones, such as citric acid. Citric acid is a mild organic acid, so it is often used in the food industry, with no negative impact on the environment, unlike the solvents conventionally used like HCl and formaldehyde. In addition, another advantage of using it in the alginate extraction process is that it is a chelating agent for metals, i.e. it provides a good ion exchange to convert alginate into insoluble alginic acid [59]. On other hand, other greener and more sustainable techniques have been developed and applied in the alginate extraction, such as UAE, which generates physical forces that lead to dispersion of the cell wall, reducing the particle size and improving the contact between the solvent and the target compounds; microwave-assisted extraction, where a microwave radiation hits the algae, radiation, heating and evaporating the water inside their cells, which leads to an increase of pressure in the cell wall and the consequent release of the compounds to the outside; enzyme-assisted extraction, where enzymes are inserted in order to react with a particular substrate or group of substrates while keeping the target products unchanged in the biomass matrix and extrusion-assisted extraction, where alginate beads and alginate-based 3D printing ink are produced with a thermo-mechanical process. Despite these techniques do not replace all the conventional process, they can be used to replace some of the steps in order to decrease the temperatures, times and toxic solvents used conventionally [54].

Some research studies already started to explore the use of more sustainable methodologies for the extraction of alginate from different algae, such as the use of ultrasound, as for example, Youssouf *et al.* reported. They developed a new process to extract alginates from brown seaweeds (*Sargassum binderi* and *Turbinaria ornata*) and carrageenans from red seaweeds (*Kappaphycus alvarezii* and *Euchema denticulatum*) with the assistance of ultrasound. The effect of several parameters (pH, temperature, algae/water ratio, ultrasound power and duration) was investigated to determine optimal extraction conditions. The extracted polysaccharides represented up to 55 % of the seaweeds dry weight and were obtained in a short time (15–30 min) as compared to 27 % in 2 h at 90 °C for conventional extraction. Ultrasound allowed the reduction of extraction time without affecting the chemical structure and molar mass distribution of alginates and carrageenan [60]. Flórez-Fernández *et al.* proposed an ultrasound assisted aqueous extraction of different compounds from *Sargassum muticum* (*S. Muticum*). Ultrasound assisted water extraction of fucoidan, phlorotannins and alginate was performed, minimized the use of chemicals, high temperatures and prolonged times. To obtain a greener process in the acid step to convert the calcium alginate to alginic acid, HCl was substituted by lemon juice, and to obtain the SA, sodium

carbonate (Na_2CO_3) was added to obtain the alginic acid sodium salt. The used sonication conditions (30 min) at room temperature (25 °C), led to the formulation of alginate gels with intermediate strength and soft mechanical properties. The authors concluded that ultrasound assisted water extraction of fucoidan, phlorotannins and alginate had an acceptable extraction yield (13.6 %), however lower than the yields obtained by conventional formaldehyde processes (25.6 %) [61]. In the same year, Flórez-Fernández *et al.* studied the non-isothermal autohydrolysis temperature impact of edible brown seaweed *L. ochroleuca*. The extraction is usually performed in acidic media for several hours, but undesirable degradation of fucoidans, lowering the fucose and sulphate content, could occur. The search for efficient and clean processes for the extraction of bioactive compounds, has led to the development of low chemical water-based systems. In this context, this work is aimed to evaluate the influence of the operational conditions during the non-isothermal autohydrolysis with the objective of solubilizing the algal biomass to recover high valuable compounds without further purification. For this purpose, the liquid phase and the alginate extracted were analyzed and studied promoting an integral use of the algae. Characterization of chemical composition, rheological features of the precipitated alginate and the activities of interest for food and non-food purposes, as a cosmetic and pharmaceutical, were also presented. The dried algal samples (60 g) were mixed into water (30:1 (w/w)) and the suspension was heated up to a 120–220 °C in a pressurized reactor equipped with a stirred vessel (3.7 L). The maximal fucose content (17 %) was attained at 180 °C, whereas the maximal sulphate was achieved at 160 °C, and phenolic and protein content at 220 °C. The maximum sulphated fucoidan content (41.38 g fucoidan/100 g extract) was obtained at 160 °C, whereas the maximum fucose oligosaccharides was obtained at 180 °C. The antioxidant capacity was equivalent to 32 mg Trolox/g dry extract produced at 220 °C. The milder processing condition was selected to study the potentiality of the precipitated alginate in terms of viscoelastic properties determined by rheology. Alginate extraction (14.94 g/100 g extract) was determined at 160 °C [62].

2.3.2 Cellulose extraction

Cellulose and its derivatives have been successfully extracted from green [63], brown [64] and red [65] macroalgae, such as *Ceramium* (18.5 %), *Chaetomorpha* (36.5-41 %), *Chondria* (16.4 %), *Cladophora* (20-45 %), *Corallina* (15.2 %), *Fucus* (13.5 %), *Gelidiella* (11.3-13.6 %), *Gracilaria* (10.5 %), *Griffithsia* (22 %), *Halidrys* (14%), *Hypnea* (11.4 %), *Laminaria* (1.1–20

%), *Rhizoclonium* (38.6 %), *Ulva* (1.8–19 %) [66]. Most reports of cellulose isolation from macroalgae are analytical studies using complex solvents, acids, bases, and sometimes enzymatic extraction procedures, and are not intended to simplify or industrialize the extraction process [67]. The most common and effective step-treatment for cellulose isolation from different sources, namely algae, is the combination of alkaline treatment, oxidative bleaching, and acid hydrolysis. During the extraction process of cellulose from algae, the non-cellulosic components must be removed [68]. The bleaching step aims to remove the lipids and pigments, to obtain highly purified, whiteness extracted cellulose. In this step, NaClO₂ and hydrogen peroxide (H₂O₂) are mainly used. The alkaline treatment uses mainly NaOH to remove the hemicellulose. Finally, the acid hydrolysis is used to cause the cleavage of glycosidic bonds through acid penetration into the cellulose fibers [64]. However, these processes generate harmful wastes, require the use of high temperatures, time, and energy, which leads to negative impact on the environment [62]. In alkaline step, due to the strong alkaline nature of NaOH, massive amount of acid/water is required to neutralize/dilute the effluent. Moreover, acid hydrolysis, with the mineral acids (HCl and H₂SO₄) has many disadvantages like difficult economic recovery of acid, the requirement of a large amount of alkali to neutralize the effluent along with the generation of with a tremendous amount of salt and low thermal stability of the extracted cellulose. Nevertheless, acid hydrolysis is the most used because of its reasonable price, lower reaction time and efficiency [49].

Thus, green, and sustainable methods have recently been explored for the extraction of cellulose and other compounds from algae [62]. Some of that examples are mechanical processes, such as micro-fluidization [69], high-pressure homogenization, and the ionic liquid treatment [70]. Wahlstrom *et al.* reported a successful extraction and characterization of cellulose from northern hemisphere green macroalgae *Ulva lactuca* (*Ulva fenestrata*). Cellulose was extracted by sequential treatment with ethanol ((85 % (v/v) for 24 h at 120 °C to remove pigments and fatty acids), H₂O₂, (4 % (v/v), at 80 °C for 16 h), NaOH, (85 % for 24 h at 120 °C), and HCl (5 % (v/v) at 30 °C for 16 h), yielding a cellulose rich insoluble fraction. The extracted cellulose was then disintegrated into lignin-free CNF using a mechanical process, without any enzymatic or chemical pre-treatment prior to the homogenization process. The obtained CNF showed characteristic peaks for the cellulose I allomorph and a crystallinity index of 48 %, confirming that the nanofibrils were semicrystalline. Characterization of the morphology of the CNF showed nanofibrils like those found in lignocellulose and regions with a sheet-like structure. About 1.1 g of extracted cellulose was obtained in the extraction starting from 50.0 g freeze-dried biomass, giving an overall yield of 2.2

% (w/w) on a dry weight basis [71]. In another study, in the attempt to use a greener method, Singh *et al.* extracted CNC from a red seaweed (*Gelidiella acerosa*) using a microwave-assisted alkali treatment. In the traditional alkali method, the solution should be heated for 2–4 h for the removal of lignin and hemicellulose. However, in this process, microwave radiation can be used as an alternative energy source, due to its ability to rapidly generate heat, and thus, reducing the process time. The bleaching and acid hydrolysis using ultrasonication were performed and the extracted CNC presented a CrI of 60 %, an extraction yield of 30 %, an average diameter of 32 nm ranging from 14 to 50 nm, and an average size of 408 nm ranging from 305-512 nm. Therefore, this method revealed to be a more efficient and greener approach for the isolation of CNC from seaweed [72].

As stated before, this project is based on the use of alginate and cellulose extracted from seaweed for biomedical applications, namely for wound dressing systems. It was said that electrospun bioactive dressings would be the best option for this application. The following section clarifies these concepts.

2.4 Electrospun algae-based nanofibers for wound healing

2.4.1 Electrospinning

Nowadays, electrospun-based wound dressings have been attracting more and more attention, since conventional treatments have failed to address the complexity of wound healing. Nanomaterials can be manipulated and adapt to accomplish the demands of acute and chronic wound healing [73]. Electrospinning is an electro-hydrodynamic technique used to produce thin polymeric fibers, patented by Cooley in 1900. The electrospinning device consists of a high-voltage power supply, a spinneret connected to a syringe pump, and a metal collector (Figure 5) [17].

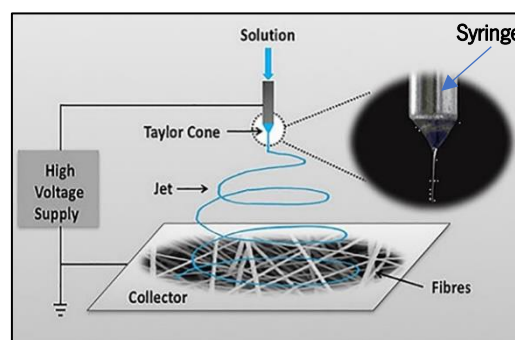


Figure 5 - Electrospinning process. Image modified from [74].

This technique is simple, straightforward, and cost-effective, with the possibility of large-scale production. Initially, a polymer solution is loaded into a syringe and is forced by a syringe pump to a needle tip. The needle is connected to a high voltage power supply so that at a specific voltage, the polymer droplet at the end of the syringe is stretched into a conical shape known as a Taylor cone. The increased electric field leads to the formation of a continuous jet that is continuously elongated and whipped by electrostatic repulsion. As the jet gets thinner, the solvent evaporates, and the nanofibers are continuously deposited in the collector. The formation of fibers from the polymer jet depends on the solution (type of polymer and its blend with other polymer(s), polymer's molecular weight and concentration; type, volatility, and concentration of the solvent(s); solution's surface tension, viscosity and conductivity), process (applied voltage, flow rate, distance between the spinneret and collector, needle diameter, and type of collector) and the environmental (temperature and humidity) parameters [17].

Regarding the solution parameters, the molecular weight of the polymers as well as the solvent used to dissolve the polymer, are very important to the final membrane, since intrinsic viscosity is related to the molecular weight of the polymer and conductivity depends on the specific solvent mixture. When the viscosity and concentration of the solution is above a certain critical value, unique for each polymer, electrospun fibers are smooth. On the other hand, when it is below this critical value, the jet is disintegrated into individual droplets. In addition, the concentration of a polymer solution affects the viscosity and surface tension. A solution with high conductivity leads to the formation of homogeneous nanofibers [73].

Considering the process conditions, the flow rate and the distance between the collector and the spinneret also need to be set within a suitable range for successful nanofiber production. When the flow rate is too low, polymer ejection is difficult to be achieved because the replacement of the solution ejected from the tip of the capillary is not sufficient, and when the flow rate is too high, beaded nanofiber formation can occur because of Taylor cone deformation. The main significance of the distance between the spinneret and the collector is related to the evaporation of the solvent after ejection of the polymer. It is necessary to provide a minimum distance so that the solvent can evaporate before reaching the collector, however, too long distances can promote other defects, such as non-uniform or sharp-beaded nanofibers [73]. Regarding the power supply voltage, the more it increases the more charges build up on the liquid droplet. If the applied voltage increases above the set point for the start of a jet, the jet elongates further, because the degree of whiplash

instability increases. Conversely, it reduces the time it takes for the charged jet to travel from the spinneret to the collector. In fact, a larger electric field can cause more likely leaks of surface charge from the jet into the surrounding environment. Consequently, the charged jet becomes unstable, resulting in defects such as beaded fibers, flat ribbon-shaped fibers, or non-uniformity in the fibers. The impact of tension on fiber formation is debatable, some research has shown that increasing applied tension reduces fiber diameter, while others say the opposite [75].

Finally, it is also important to consider environmental parameters, such as temperature and humidity. An increase in temperature promotes a decrease in the viscosity of the polymer solution, and consequently, a decrease in the diameter of the electrospun nanofibers. The effect of relative humidity on electrospinning has been shown to depend on the molecular interactions between the polymers and solvents used, which affects the evaporation rate of the solvent, and consequently the final fiber morphology [73].

The electrospinning technique is now used to manufacture ultra-thin fibers with diameters between 50-500 nm, which allows them to mimic natural ECM fibers (since the porous cross-linked collagen fibers found in the native ECM also have diameters between 50 and 500 nm [76]), one of the main benefits to be used for wound dressing. In addition, it offers advantages such as increased adaptability to the wound environment, encapsulation and delivery of biopharmaceuticals, ability to allow gas exchange between the wound and the surrounding environment, absorption of wound exudates, and the possibility of surface functionalization to further promote biocompatibility and active properties (e.g., antimicrobial activity) [18]. The highly interconnected pore structure with reduced pore size act as a barrier to prevent the microbial penetration as well as to allow water and oxygen permeability between the wound and the surrounding environment [9]. Moreover, the possibility of incorporating bioactive agents with an active role in the healing process, demonstrates the great potential of the electrospun membranes to act as active dressings [9]. There are multiple strategies for incorporating drugs into electrospun fibers, including blend electrospinning, emulsion electrospinning, coaxial electrospinning, and surface immobilization [77],[9],[77], as shown in Figure 6.

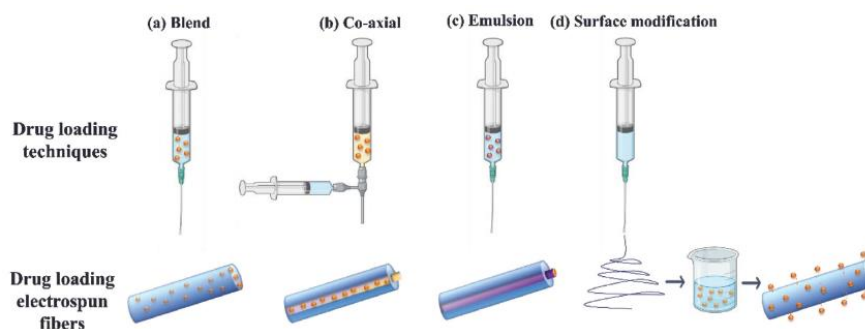


Figure 6 - Different techniques for drug incorporation by electrospinning. Image from [9].

In the next section some examples of nanofibers made by electrospinning with SA for biomedical applications, some of them for wound dressing, will be analyzed in order to show the potential of these fibers to act as drug delivery systems for wound dressing.

2.4.2 Alginate-based electrospun membranes as wound dressing systems

As already mentioned, alginates are non-toxic, biostable hydrophilic polymers with stabilizing, thickening, and emulsifying properties, which in the presence of divalent cations, form a water-insoluble gel that is thermo-irreversible. Moreover, there are studies indicating that they lower blood pressure and cholesterol levels, prevent the absorption of heavy metals in the body, contribute to the prevention of diabetes and adiposity. For those and more reasons, alginates constitute biomaterials with several applications in the biomedical sector, namely for wound dressing as they can absorb wound fluids and promote the wound healing process [41].

The development of electrospun nanofibers with SA alone is quite difficult due to its polyelectrolyte nature having high conductivity, lack of chain entanglements, high surface tension of the spinning solutions [41], rigid intramolecular and intermolecular hydrogen network and gelatinous nature [78],[79]. So, one of the methods to overcome these drawbacks is to blend the polysaccharide with a compatible electrospinnable polymer, including synthetic polymers, like PVA or PEO [80]. There are reports where they use synthetic polymers such as PVA and PEO. PVA is one of the most used polymers in the biomedical field, in particular for the fabrication of nanofibers membranes based wound dressings [81], [79], because it is non-toxic, water-soluble, biocompatible, chemical resistant, biodegradable and has good fiber forming ability. Moreover, the thermal stability and mechanical properties of electrospun membranes can be improved after the

blending of PVA and SA due to the formation of hydrogen bonds between the two polymers. Furthermore, different bioactive compounds can be added in order to improve or create other properties, including antimicrobial activity [78].

There are several studies showing the successful development of electrospun membranes with SA/PVA for wound dressing systems and other applications. Table 1 reports some of these studies, demonstrating the concentrations of the polymers and their optimal ratio, the incorporated bioactive compounds as well as the electrospinning parameters (distance between the needle and the collector (D), voltage (V), flow rate (FR) and the needle diameter (Dn) and the diameters of the developed nanofibers). It is important to note that all these studies used commercial SA. However, they are important to demonstrate the potential of these fibers composed by SA and PVA for wound dressing.

Table 1: Examples of SA/PVA electrospun nanofibers for wound dressing systems.

| SA (%) | PVA (%) | Optimal Ratio SA/PVA | Compound | Electrospinning Parameters | Diameters (nm) | | Applications | Ref. |
|--------|---------|----------------------|--|---|----------------|-----------------|---|------|
| | | | | | SA/PVA | SA/PVA/Compound | | |
| 2 | 12 | 4:6 | Moxifloxacin hydrochloride (MH) (antibiotic) | D = 10 cm V = 14 kV FR = 0.3 mL/h Dn = 0.7 mm | 148 ± 41 | 175 ± 75 | Wound dressing | [82] |
| 0.8 | 7.2 | - | Honey | D = 10 cm V = 15 kV FR = 0.4 mL/h Dn = 0.5 mm | 379 ± 65 | 528 ± 160 | Wound dressing | [83] |
| 2 | 10 | 3:7 | Gatifloxacin (GH) (antibiotic) | D = 10 cm V = 20 kV FR = 0.1 mL/h Dn = 0.7 mm | - | - | Drug delivery for wound healing | [84] |
| 2 | 16 | 1:1 | Zinc oxide (ZnO) nanoparticles | D = 5 cm V = 17 kV FR = 0.1 mL/h Dn = 0.723 mm | 190-240 | 220-360 | Antibacterial wound dressing | [85] |
| 2 | 14 | 1:2 | Nano-hydroxyapatite (nHAP) | D = 17 cm V = 20 kV FR = 0.32 mL/h Dn = 0.510 mm | 350 | 270 | Tissue regeneration material | [86] |
| 2 | 16 | 8:2 | Naftifine (NFT) (fungicide) | D = 15 cm V = 15 kV FR = 1 mL/h Dn = 0.7 mm | 242.46 ± 63.74 | 457.71 ± 134.88 | Topical antifungal drug delivery system | [87] |

| | | | | | | | | |
|---|---|-----|------------------|--|-----|-----|--|------|
| 3 | 8 | 2:8 | Chitosan coating | D = 15 cm V = 16 kV FR = 0.6 mL/h Dn = 0.6 mm | 159 | 164 | Removal of Arsenic (As) from potable water | [88] |
|---|---|-----|------------------|--|-----|-----|--|------|

For example, in the study performed by Fu *et al.*, electrospun MH/PVA/SA nanofibers to act as antibacterial wound dressing were developed. In order to prove the potential of this dressing in wound treatments, *in vitro* and *in vivo* tests were developed. For the *in vivo* tests, four wounds were created on the dorsal of four rats. Figure 7 shows the representative images of wound healing with the developed nanofibers in different days [89].

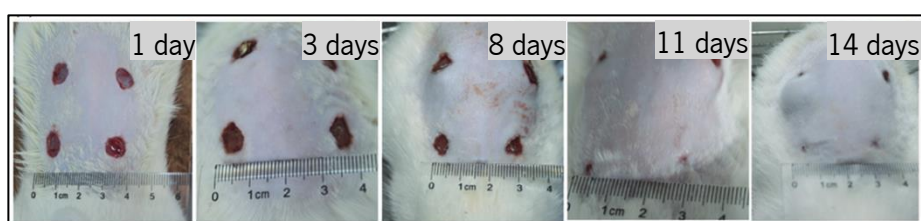


Figure 7 - Picture of rat wound dressing experiment at 1, 3, 8, 11 and 14 days after injury. Image modified from [89].

Wound closure was observed in all groups (treatment, control group, negative control group and blank control group) within 14 days after surgery, however healing in the treatment group was noticeably faster than in the other three groups. In addition, swelling and inflammation were observed in the wounds of the untreated group that were not observed in the group with treatment. The MH/PVA/SA fiber mat was showed a high swelling capacity and low weight loss of the nanofiber. This is an important property for wound care, as it controls wound exudate and maintains a moist wound environment. Furthermore, in the SA/PVA and untreated groups granulation tissue formation was observed, characterized by the accumulation of non-specific inflammatory cells. On day 14, it was observed that epithelialization was completed after treatment with the MH/PVA/SA nanofibers. The epidermis in the PVA/SA nanofiber and control groups was not yet partially closed and skin dependencies were still barely visible in these groups. Furthermore, it was concluded that MH/PVA/SA nanofibers had excellent *in vitro* biocompatibility at the tested concentrations (0.2-0.8 mg/mL) using L929 cells. Overall, these results showed that the SA-based membranes containing MH are a promise approach to increase the effectiveness of wound dressings [82].

For the same applications, Tang *et al.* developed a promising SA/PVA electrospun nanofiber incorporated with honey. The results showed that the nanofibers without honey had a smooth morphology and homogeneous size compared to those with 20 % (v/v) honey, which had a more non-uniform morphology with a wider distribution of nanofiber diameters. One of the most important properties of a wound dressing is water absorption capacity, reflecting the ability to absorb exudates during the wound healing process. Thus, in this study SA/PVA nanofibers without honey showed better maximum water absorption capacity than those with honey. Such results showed that the honey content of nanofibers should be well considered and adjusted according to different applications. Furthermore, it was found that with increasing honey content in the nanofibers, the antibacterial activity was enhanced against *E. coli* and *S. aureus*, which is favorable for the wound healing process. However, nanofiber membranes without honey showed no antibacterial activity against these bacteria after 24 h of incubation. Antioxidant activity is another beneficial property concerning inflammation of wounds. It was found that with the increasing of honey content, the antioxidant activity also increased, with the membrane with 20 % honey having the best activity. The SA/PVA nanofiber membrane without honey also showed antioxidant activity, however weaker, which correlates mainly with the antioxidant capacity of SA. Regarding cytotoxicity, both nanofibers with or without honey showed high viability, exceeding 93 %, which demonstrates the good biocompatibility of honey/SA/PVA and SA/PVA nanofibers. Therefore, honey/SA/PVA nanofibrous membranes could be a promising candidate as an effective wound dressing [83]. With the studies analyzed, it is possible to conclude that the membranes with SA/PVA have good properties for wound dressing, namely, the ability to absorb wound exudate, antioxidant activity and a good cellular compatibility, i.e. a good biocompatibility. However, regarding antibacterial activity, it is not developed with only SA/PVA nanofibers, so it will always be necessary to add a compound, such as those reported, to add this property [83]. In a similar study, Shalumon *et al.* prepared SA/PVA/ZnO nanofibers for wound dressings, with antibacterial activity, where an optimum amount of ZnO was obtained for which the toxicity is minimal and the antibacterial activity maximum. SA/PVA/ZnO electrospun membranes demonstrated antibacterial activity against *S. aureus* and *E. coli* and good cell adhesion and spreading. However, as the concentration of ZnO nanoparticles increased, a lack of cell dispersion and consequent change in cell morphology was observed. This may be associated with the slightly toxic effect of the ZnO nanoparticles at higher concentrations. The cytotoxicity study of SA/PVA mat with and without ZnO was also performed with L929 cells. Both showed positive results, showing that the polymer blend is not cytotoxic [85].

Furthermore, SA/PVA nanofibers also show a promising offer to act as drug delivery systems, as Arthanari *et al.*, shown in their study. They developed SA/PVA/GH electrospun nanofibers, which proved to successfully control the rate and period of drug release in wound healing applications, since the *in vitro* release profile of nanofibers shows a controlled continuous release of the drug within 6 h . Furthermore, there was a decrease in the swelling of the nanofibers with the drug, which may be due to the water solubility of the drug [84].

Although there are almost no published studies where the SA extracted from algae is directly used for the development of nanofibers by electrospinning, it has been proven that the SA can be extracted from algae and that the SA can be used successfully for the development of electrospun nanofibers to act as wound dressing. Thus, this project aims to arrive at a green and sustainable process for extracting SA from algae and then using this same SA to develop electrospun nanofibers.

2.4.3 Natural extracts

As verified, there are several bioactive compounds that can be incorporated into electrospun nanofibers, in order to create new functional properties, such as antimicrobial activity. In recent years, alarming emergence of antimicrobial resistance in pathogens have posed a challenge to health and food production worldwide. Traditional strategies used for antibiotic discovery persist, resulting in the re-isolation of known compounds, necessitating the need to develop new strategies to treat infections associated with antibiotic-resistant microorganisms. Notably, analysis of the new chemical entities identified over the past 40 years has revealed that compounds based on natural products remain the primary source of antibacterial compounds [89].

Zizyphus, is a natural extract, that belongs to the family of *Rhamnaceae* and has been used in traditional medicines due to its nutritive and remarkable biological properties [90]. Normally it 's used as tonic and aphrodisiac and sometimes as hypnotic-sedative and anxiolytic, anticancer (Melanoma cells), antifungal, antibacterial, antiulcer, anti-inflammatory, antispastic, antinephritic, cardiogenic, antioxidant, immunostimulant, and present wound healing properties. Pharmacological screening studies indicated that the extract of *zizyphus* leaves contains beutic acid and ceanothic acid, cyclopeptides, as well as flavonoids, lipids, protein, free sugar and mucilage and four saponin glycosides: christanin A, christanin B, C and D. It well reported that the extract of *zizyphus* exhibited anti-nociceptive potency and may prevent chronic alcohol-induced liver injury by enhancing the levels of total antioxidant status and inhibiting hepatic lipid peroxidation

[91]. Therefore, the incorporation of this natural extract into electrospun nanofibers could provide new active properties to the membranes, which can be useful to enhance the healing process.

3. MATERIALS AND METHODS

In this work, processes for extracting alginate and nanocellulose from different algae were developed and optimized, in order to find the greenest and most sustainable processes possible, as well as the development of electrospun nanofibers. This section describes the materials used, namely which algae and solvents were used. Furthermore, the processes used, and their optimization are described. Lastly, the methods used for the characterization of the obtained samples will also be presented.

3.1 Materials

Three types of algae provided by CIIMAR (Interdisciplinary Center for Marine and Environmental Research) in Portugal, were used for the extraction of alginate and/or nanocellulose: *L. ochroleuca*, *Sargassum Muticum* (brown algae) and *Ulva* Spp. (green algae). Several solvents were used for the extraction processes: hydrochloric acid (HCl), water (H₂O), ethanol, sodium carbonate (Na₂CO₃), citric acid, calcium chloride (CaCl₂), sulfuric acid (H₂SO₄), peroxide hydrogen (H₂O₂), sodium hydroxide (NaOH), and acetone. For the development of electrospun nanofibers PVA was used. The specifications of each of them are shown in Table 2. Additionally, for comparison purposes, commercial alginate from Sigma Aldrich, was used.

Table 2: Characteristics of the materials used in this work.

| Solvent | Brand | Molar mass or Concentration |
|--------------------|-------------------|-----------------------------|
| Hydrochloric acid | Tritisol | 1 mol/l |
| Ethanol (96%(v/v)) | Aga | 96 % (v/v) |
| Calcium chloride | Panreac | 110.99 g/mol |
| Sodium hydroxide | Normax | 1 mol/l |
| Citric acid | Sigma- Aldrich | 192.12 g/mol |
| Sodium Carbonate | JMGS | 105.99 g/mol |
| Peroxide Hydrogen | Normax | 34.01 g/mol |
| Sulfuric Acid | PanReac AppliChem | 98.08 g/mol |
| Sodium Alginate | Sigma-Aldrich | - |
| PVA | Polysciences | |

Figure 8 shows the electrospinning equipment used in this work (MECC NF-103). Similar to the other electrospinning equipment, it is composed of a high voltage source, a syringe pump and a collector. Moreover, it has a control panel that allows manipulating the operating conditions, namely, the distance between the needle and the collector, the applied voltage and the flow rate. The polymer solution was placed in a 20 mL syringe and a needle with a diameter of 0.61 mm was used. The capillary tube used was 30M tube flexene, 1.6x3.2MM, 971692, BLUE PT_A_DHE. Only one type of collector was used for the production of the fibers, a static one (metal plate covered with aluminum foil).

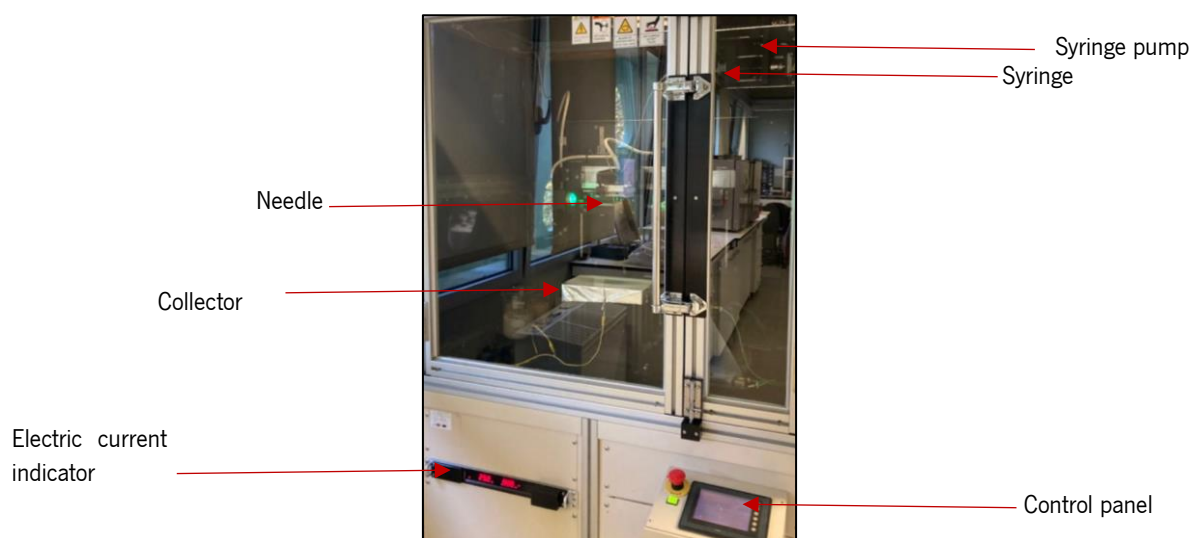


Figure 8 - Electrospinning equipment used in this work.

3.2 Methods

3.2.1 Optimized process for the extraction of alginate from algae

Three different methods for extracting alginate from algae were performed and evaluated, and in this section only the most successful method will be presented. In the next section, the other methods (Process 1 and 2) will be presented with their analyses and optimizations. The optimized extraction process will be designated as Process 3. This extraction process was performed based on the methods presented in the paper of Trica *et al.* [92] and Fertah *et al.* [93], with some modifications. The method consists in first grind the seaweed into powder, followed by a depigmentation/delipidization step, an acid treatment, a basic treatment, a precipitation, washing and in a drying step. Initially, 5 g of *L. ochroleuca* dried seaweed was ground and the resulted powder was soaked in ethanol (96 % (v/v), 24 h, 160 mL) in order to remove phlorotannins and

pigments. The solid part was removed by filtration with a metal filter, washed with distilled water, and added to HCl (0.2 M, 24 h, 160 mL). The excess acid was washed away with distilled water before extracting the alginate in a Na₂CO₃ solution (2 % (w/v), 3 h). The SA extract was separated from the solid waste by centrifugation (15 min, 5000 rpm). SA was precipitated with ethanol (96 % (v/v), 160 mL). Finally, SA was purified with ethanol and acetone before being dried in oven at 50 °C for 24 h. The acidic pretreatment is usually performed using mineral acid (HCl or H₂SO₄), but in an attempt to make the method greener and more sustainable, considering that it is also one of the goals of this project, the HCl in the acid treatment process was replaced by a weaker or milder acid, citric acid (0.2 M, 24 h, 160 mL) [94], [95]. The process was then repeated with a larger quantity of initial algae (25 and 40 g), and adapting the amounts of solvents used, showing the scalability and reproducibility of this methodology. Figure 9 represents the different steps performed during the extraction of SA using the Process 3.

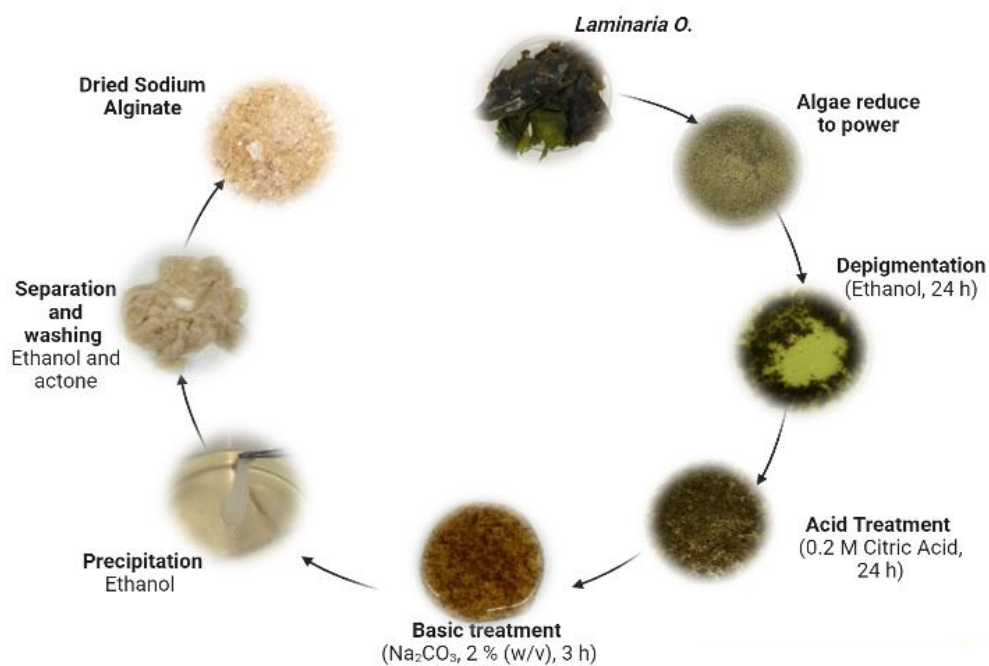


Figure 9 - Schematic diagram of the optimized Process 3 for extraction of SA from *L. ochroleuca* algae.

3.2.2 Nanocellulose extraction process

For the extraction of nanocellulose, *Ulva* spp. algae was used. The first attempt for nanocellulose extraction was based on the methodology described by Chen *et al.* [72], with some modifications, as shown in Figure 10.

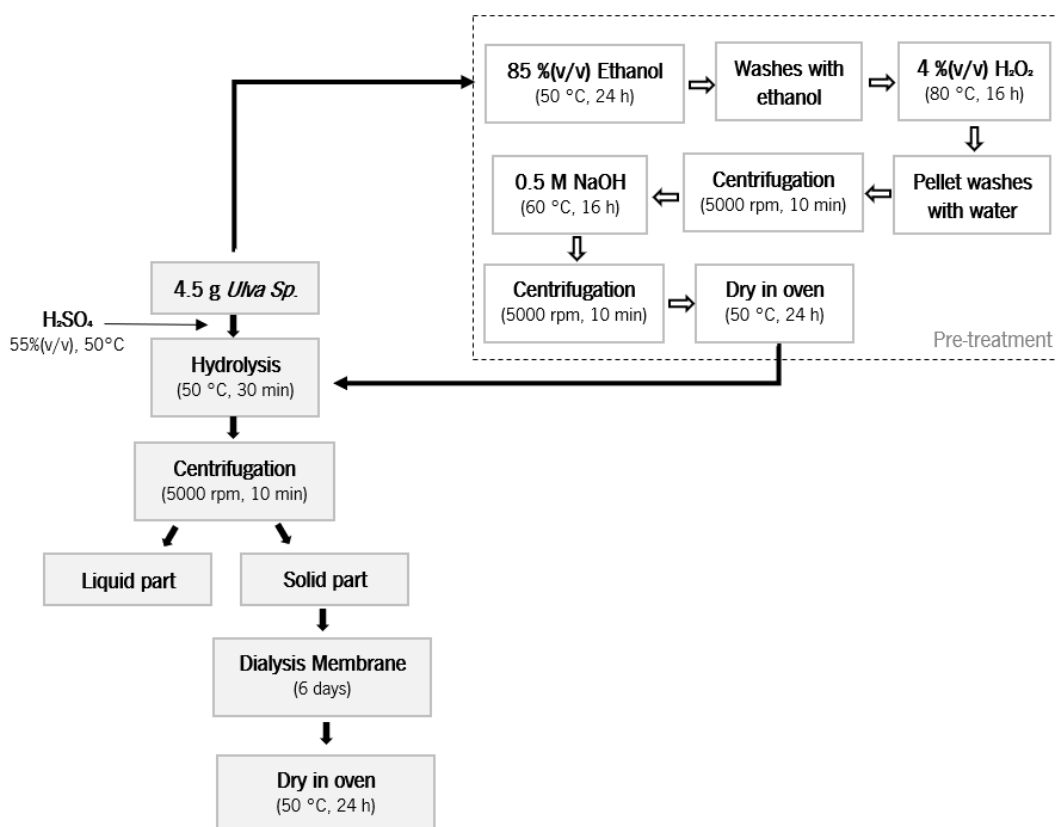


Figure 10 - Schematic diagram of method used for the extraction of nanocellulose from *Ulva* spp. algae.

Ulva spp. was first converted into powder using a mortar. The powder (4.5 g) was added to a solution of 150 mL 55 % (v/v) H₂SO₄ at 50 °C and left under stirring in a double-neck round-bottom flask for 30 min. This solution was put under reflux, as shown in Figure 10. After that, in order to stop the hydrolysis, water was added, and the solution was then centrifuged at 5000 rpm, 10 min, and washes with water were performed in order to reach a pH of 5.5. Finally, the pellet was collected and placed on a dialysis membrane (33 mm x 21 mm MW06245) for 6 days, in order to increase the pH and allow exchanges with the water. The water was changed every day to not become saturated and not to hinder the exchanges. After this procedure, the content of the membrane was poured and dried in the oven at 50 °C.

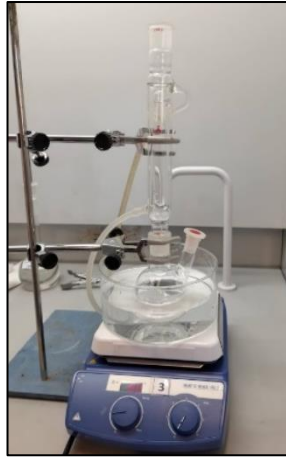


Figure 11 - Assembly for the extraction of nanocellulose from *Ulva* spp. algae using acid hydrolysis (H_2SO_4).

In a second approach, a bleaching pre-treatment was performed, based on the treatment performed by Wahlstrom *et al.* with some modifications [96], in order to purify the algae before extraction. This pre-treatment consisted of placing 4.5 g of algae reduced to powder, in ethanol (85 % (v/v)), at 50 °C, for 24 h. Subsequently, the pre-treated algae were washed with ethanol twice and placed in the oven to dry for 24 h at 50 °C. Then the sample was resuspended with H_2O_2 (4 % (v/v)) at 80 °C for 16 h. It was allowed to cool, centrifuged at 5000 rpm for 10 min, and the supernatant was discarded. The pellet was washed with water until it reached pH 7. Afterwards, pellet was added to a solution of NaOH (0.5 M) at 60 °C for 16 h, followed by centrifugation (5000 rpm, 10 min) until it reached pH 7, and finally placed in the oven at 50 °C. After this pre-treatment, acidic hydrolysis was performed in the same way as described above.

3.2.3 Determination of the minimum inhibitory concentration (MIC) and the minimum bactericidal concentration (MBC) of the natural extract of *Ziziphus*

In order to use the natural extract *Ziziphus* leaves as antibacterial compound to be incorporated into electrospun membranes, the determination of MIC and MBC was performed. Bacterial inoculate were prepared from a single colony of *S. aureus* (ATCC 6538) and incubated overnight at 37 °C and 150 rpm under aerobic conditions in Tryptic Soy Broth (TSB) medium. Bacterial suspensions were prepared at an initial concentration of 5.0×10^5 CFU/mL in MHB. Different solutions of the extract (40.960; 36.864; 32.768 and 24.576 mg/mL) were prepared, in distilled water, and added to the first column of 96-well plates, in a volume of 100 μL . Serial

dilutions (1:2) were made with MHB in the consecutive wells, for a final volume of 50 μ L. Then, to each of the wells, 50 μ L of the bacterial suspensions were added. The bacterial suspensions without extract and the culture medium were used as negative and positive control, respectively. To determine the MIC of the extract, the differences in absorbance readings (between 0 and 24 h) were analyzed and an attempt was made to find the concentration at which the bacteria showed no growth (Figure 12).

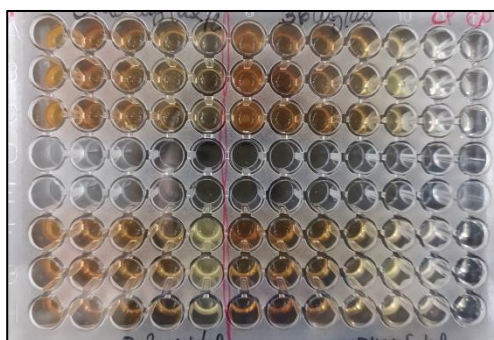


Figure 12 - Well plate for MIC determination after 24 h.

Subsequently, the determination of MBC against *S. aureus* bacteria was performed. *S. aureus* are one of the most common bacterial species that cause wound infections, as they find a suitable environment for colonization and proliferation in the deeper tissues of the skin. Furthermore, they are considered to be antibiotic-resistant microorganisms, being among the most dangerous resistant to vancomycin [97].

3.2.4 Development of alginate-based electrospun nanofibers

Preparation of electrospinning solutions

The SA extracted from *L. ochroleuca* algae was used to produce the polymeric solutions to be used in electrospinning. PVA was blended with SA in order to enable its electrospinnability. Initially, two aqueous solutions containing 4 % (w/v) of SA and 16 % (w/v) of PVA were prepared and left under stirring at 50 °C for 24 h. Then, SA solution and PVA solution were mixed with different ratios (SA/PVA): 50:50, 60:40, 70:30, 80:20, 90:10 for 2 h.

In a second step, 1.25 mg/mL of the natural extract *Ziziphus* was incorporated into the solution of SA/PVA (50:50), and was stirred for 1 h at room temperature, considering the MBC values determined.

Electrospinning Process

For the electrospinning process, after several parameters tested, the optimized ones were: 20 mL syringe with a stainless steel needle, with 0.61 mm of diameter, was filled with the blend solution and mounted onto a syringe pump working at a constant flow rate of 0.2 mL h⁻¹. The needle was clamped to the positive electrode of a high voltage supply generating 22 kV, and the grounded electrode was connected to an metallic collector covered with aluminum foil (tip-to-collector distance was 14 cm). The electrospun membranes were produced with 2 h of deposition. The temperature and humidity conditions were properly controlled, ranging from 20 to 25 °C and 60 and 65 %, respectively. Table 3 shows the optimized parameters used to develop the electrospun membranes.

Table 3: Optimized electrospinning parameters to produce SA/PVA and SA/PVA/ *Ziziphus* electrospun nanofibers.

| | |
|---------------------------------------|------------------------|
| D _{needle} | 0.61 mm |
| Deposition time | 2 h |
| Voltage | 22 kV |
| Flow Rate | 0.2 mL h ⁻¹ |
| Distance between needle and collector | 14 cm |

3.3 Characterization methods

3.3.1 Evaluation of the viscosity of the polymeric solutions

The viscosity of the solutions used for electrospinning were measured using Myr's VR3000 rotary viscometer, which allows viscosity measurement in an efficient and practical way. The measurement of the solutions was performed using the R4 spindle and a speed of 50 rpm.

3.3.2 Extraction yield

Extraction yield was calculated by equation (1) according to [98].

$$YIELD (\%) = \frac{\text{Weight of alginate}}{\text{Weight of seaweed dried biomass}} \times 100 \quad (1)$$

3.3.3 UV-visible spectroscopy

Ultraviolet visible (UV-Vis) spectrophotometers use a light source to illuminate a sample, with light across the UV to the visible wavelength range. The instruments then measure the light absorbed, transmitted, or reflected by the sample at each wavelength. From the obtained spectrum, it is possible to determine the chemical or physical properties of the sample [99]. UV-Vis absorption spectra of the different samples were obtained using a Shimadzu UV-1800 spectrophotometer equipped with quartz cuvettes with a 1 cm of optical path. Each spectrum was acquired at a wavelength between 200 and 450 nm. The UV-Vis spectrum of each sample was obtained as well as the one of commercial alginate, for comparison purposes. The samples were diluted in water to avoid deviation from the linearity of the Beer-Lambert law.

3.3.4 Attenuated Total Reflectance - Fourier Transform Infrared Spectroscopy (ATR-FTIR)

ATR-FTIR is a technology used for the chemical characterization of materials at the molecule level. In active infrared transitions, the electric dipoles of vibrating functional groups change as they absorb incoming infrared light, and these are plotted as a function of wavenumber, in cm^{-1} [100].

ATR-FTIR was performed in an IRAffinity-1S equipment, SHIMADZU (Kyoto, Japan), equipped with an ATR accessory, and it was used to analyze the SA and nanocellulose extracted from algae. Each spectrum was acquired in transmittance mode in a diamond ATR cell by accumulation of 45 scan cycles and with a resolution of 4 cm^{-1} . The equipment was programmed to read the transmittance of the samples in a spectrum from 400 to 4000 cm^{-1} . The samples were analyzed in different locations to ensure homogeneity.

3.3.5 Optical microscopy

Optical microscope uses visible light and a system of lenses to magnify images of small samples. Their images can be captured by normal light-sensitive cameras to generate a micrograph [101]. In this work, the optical microscope Leica DM750 M (bright-field) was used to analyze the nanocellulose extracted from algae and the alginate-based electrospun membranes. This microscope consisted of a system of two eyepieces and five objectives (5x, 10x, 20x, 50x and 100x).

3.3.6 X-Ray Diffraction (XRD)

XRD is a characterization technique, which evaluates material's properties such as crystal structure and crystallite size. XRD is based on the principle of the Bragg equation, which is described in terms of reflection from the incidence of collimated X-rays on a crystalline plane of the sample to be characterized. An X-Ray beam is passed through the sample and is scattered, or diffracted, by the atoms in the path of the investigated X-Rays. The interference that occurs due to the scattering of the X-Rays from each other is observed by applying Bragg's law and a properly positioned detector, and the characteristics of the crystalline structure of the material are determined. All measurements are performed in Angstroms ($1 \text{ \AA} = 0.1 \text{ nm}$ or 10^{-10} m) [102]. This technique was performed using a Bruker D8 Discover diffractometer, with a voltage of 40 kV and a current of 40 mA, with Cu-K β radiation. Data were collected for values of 2θ ranging from 5° to 45° .

3.3.7 Thermogravimetric Analysis (TGA)

TGA is a technique for measuring the thermal stability of materials. In this method, changes in the weight of a specimen are measured while the temperature is increased. The TGA graph usually shows the weight loss (%) in relation to increasing temperature, showing that the mass of the sample is continuously changing according to the heat treatment [103]. TGA analysis was performed using a STA 700 SCANSCI equipment, under nitrogen atmosphere, in the range of temperatures from 30 to 600 °C. and a heating rate of 10 °C/min.

3.3.8 Field Emission Scanning Electron Microscopy (FESEM)

FESEM is a powerful visualization tool that provides a three-dimensional (3D) image with high resolution and is used to characterize the morphology of the sample surface, particle size, microorganism, and fragments [104]. In this work, FESEM (NOVA 200 Nano SEM, FEI Company (Hillsboro, OR, USA)) was used to analyze morphologically the fibers produced by electrospinning. The samples were pre-coated with a very thin (20 nm) Au-Pd film (80-20% (w/v)) using a spray coating apparatus, 208 HR Cressington Company (Watford, UK), coupled to a high-resolution Cressington MTM-20 coating thickness controller. Secondary electron images, i.e., the topographical images, were taken at an accelerating voltage of 10 kV. The images were processed with the *ImageJ* tool in order to analyze the diameters of the obtained nanofibers.

4. RESULTS AND DISCUSSION

4.1 Alginate extraction from algae

4.1.1 Optimization of alginate extraction process

As already mentioned, three procedures were performed for the extraction of alginate from algae, and the third procedure (Process 3) showed the most promising results. Next, the results of each of these attempts will be analyzed and discussed.

PROCESS 1

The first attempt for alginate extraction was based on the methodology described by Flórez-Fernández *et al.* [61], with some modifications. Firstly, 3 g of algae *Sargassum Muticum* in form of powder was soaked in 60 mL of water and placed in an ultrasound bath for 45 min. Ultrasound assisted aqueous extraction was used in order to minimize the use of chemicals, high temperatures and prolonged times. Afterwards, it was centrifuged at 4500 rpm for 10 min, resulting in a biphasic solution, where the liquid part was placed overnight at 4 °C. Then, the liquid part was centrifuged at 4500 rpm for 20 min, in order to obtain a liquid phase alginate free and alginate fraction. Next, in order to obtain the alginic acid, citric acid (1 M) was added to the pellet (alginate fraction) and stirred for 2 h. Finally, Na₂CO₃ (1 % (w/v)) was added to obtain the SA. Figure 13 represents a scheme of the process.

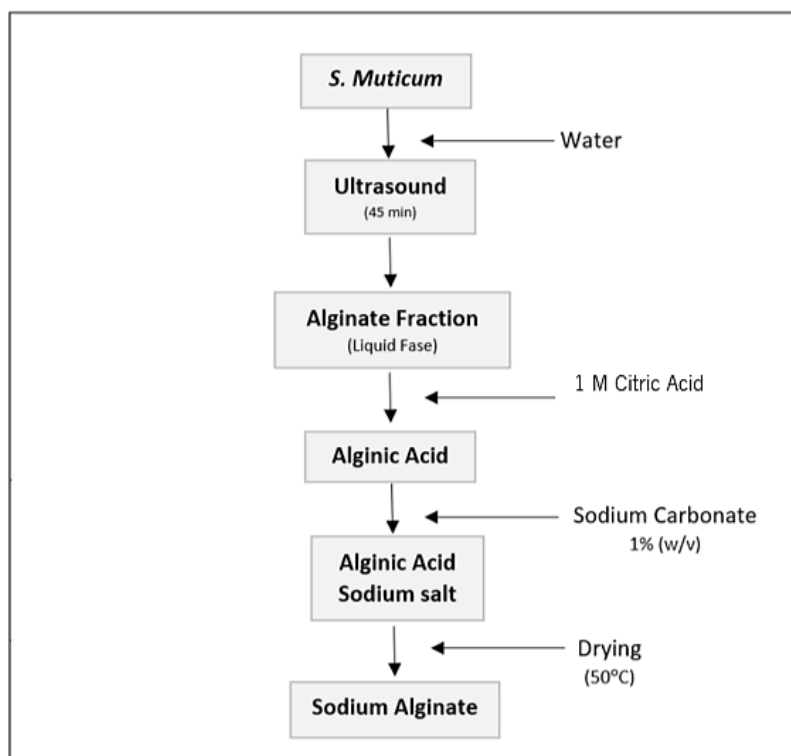


Figure 13 -_Scheme of Process 1 for alginate extraction.

However, this process 1 of alginate extraction did not allow the formation of any precipitate, i.e. a solid sample. There was no precipitate may be due to the lack of an essential step in the extraction process that is not reported in the paper on which this method was based, namely the step of precipitation of the SA with ethanol or other solvent.

PROCESS 2

Another extraction process, based on the methodologies described by A. Lorbeer *et al.* and Youssouf *et al.* [60], was evaluated with some modifications [105]. Firstly, 50 g *L. ochroleuca* was ground down to a powder, and then immersed in 150 mL ethanol, which was left under stirring for 24 h. After that, the solution was placed in ultrasound bath for 1 h. After this time, vacuum filtration was performed, and the solution was washed twice with distilled water. Subsequently, in order to extract the alginate, 2 % (w/v) of Na₂CO₃ (300 mL) was added, and left under stirring for 3 h, and then centrifuged for 10 min at 4200 rpm, leaving a biphasic solution. Finally, 20 mL of ethanol was added to the supernatant resulting from the centrifugation, to precipitate the SA. The solution was filtered to collect all the solid fraction and dried overnight at 50 °C. After drying, the obtained alginate was reduced to dust. Finally, the obtained powder was weighed and the extraction yield was calculated according to equation 1.

In order to optimize this process, the same procedure was repeated, only changing the filtration method and the amount of ethanol added. The vacuum filtration caused a lot of waste and it took about 3 h to be completed, so it was replaced by a metal filter, decreasing the filtration time and the waste generated. The amount of ethanol was increased from 20 to 80 mL to form as much alginate as possible. Figure 14 shows the scheme of this process for alginate extraction. Figure 15 shows some steps of this process.

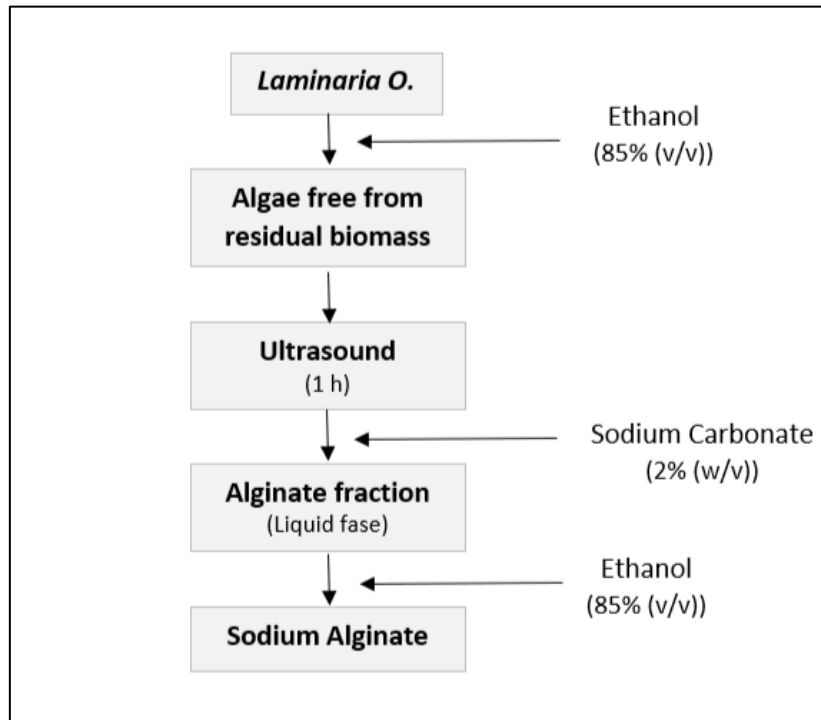


Figure 14 - Scheme of Process 2 for alginate extraction.

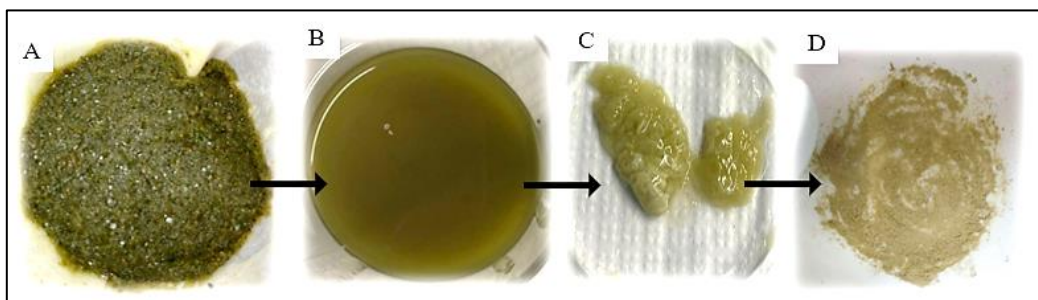


Figure 15 - Process 2 for alginate extraction from *L. ochroleuca*. **A)** Algae after ethanol treatment and filtrations. **B)** Supernatant after Na_2CO_3 addition and centrifugation. **C)** Filtered alginate after ethanol addition. **D)** Dried alginate in powder form.

Extraction Process 2 was firstly evaluated in terms of yield, according to equation 1. Using *L. ochroleuca*, it was achieved a yield of 17.8 %, with an initial mass of 5 g and a final mass of 0.8915 g. Nevertheless, the extraction yield is considered low compared with literature, (Table 6). In order to characterize the alginate extracted from *L. ochroleuca*, ATR-FTIR was performed. Figure 16 shows the spectra of the SA extracted and the commercial one.

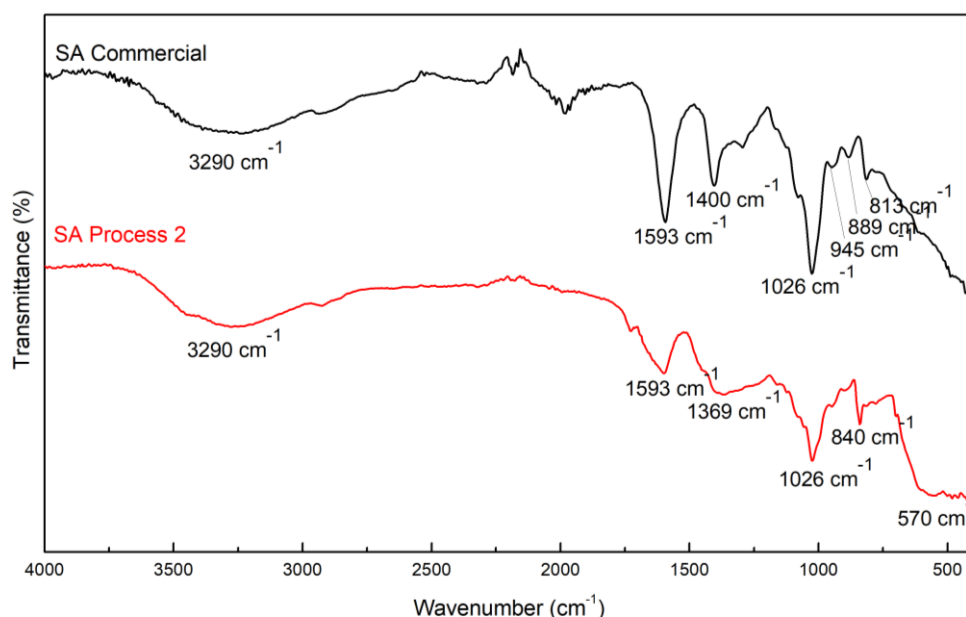


Figure 16 - ATR-FTIR of the commercial SA and the extracted SA from *L. ochroleuca* algae using the extraction Process 2.

The spectra of SA extracted with Process 2 and commercial SA showed some similar bands, like the characteristic band at 3290 cm⁻¹, which corresponds to O-H stretching, the bands at 1593 cm⁻¹, correspondent to carboxylate O-C-O asymmetric stretching vibration and to C=O asymmetric stretching vibrations of uronic acids, with a weaker intensity in the spectrum of extracted SA. The peak at 1400 cm⁻¹, that can be attributed to C-OH deformation vibration and the peak at 1026 cm⁻¹, which is related to C-O and C-C stretching vibrations of pyranoses, with reduced intensity in the extracted samples [58], [93]. Nevertheless, the spectra of commercial SA showed a band at 889 and 813 cm⁻¹, assigned to mannuronic and guluronic acids respectively. They are also attributed to C-H deformation of β -mannuronic acid and stretching vibrations of C-O with contributions from stretching of C-C and deformation vibrations of C-C-O of mannuronic and guluronic acids. Moreover, SA commercial also shows a band at 945 cm⁻¹, indicative of uronic acid presence by the C-O stretching vibration [106]. The extracted SA does not show these characteristic SA bands, it only shows one at 840 cm⁻¹ that can be attributed to mannuronic acid. In addition, the spectrum of the extracted SA shows a band that is absent in the commercial one, at 570 cm⁻¹ that may be attributed to sodium carbonate [107], which may have been left unwashed, suggesting that the final washing process should be carried out differently.

Overall, it can be concluded that the extraction of SA from *L. ochroleuca* algae was successfully performed using the extraction Process 2. However, the obtained yield was quite low,

which can be probably because no acid was used in the extraction step, which was replaced by ultrasound. Therefore, the optimization of this process was performed in order to obtain higher extraction yields (Process 3).

4.1.2 OPTIMIZED PROCESS – PROCESS 3

I. Extraction Yield

The extraction Process 3 using citric acid was the most efficient process in terms of yield, achieving a maximum yield of 39.60 %, with an initial mass of 5 g of algae, and a final mass of alginate of 1.98 g. Regarding the extraction made with HCl, the yield was 35.07 %, with an initial mass of 5 g and a final mass of 1.75 g. Table 4 shows some studies of conventional alginate extraction processes and other more sustainable ones, as well as the yield obtained, in order to make a comparison between these two and between these and the one developed in this project.

Table 4: Yield obtained in conventional and green alginate extraction process.

| Species | Yield (%) | Extraction Process | Ref. |
|----------------------|-----------|--|-------------|
| <i>L. ochroleuca</i> | 28.96 | Acid extraction with formalin and HCl solution | [108] |
| <i>L. ochroleuca</i> | 27.50 | Acid extraction with formalin and HCl solution | [109] |
| <i>L. ochroleuca</i> | 13.60 | Non-isothermal autohydrolysis | [110] |
| <i>L. ochroleuca</i> | 17.30 | Hydrothermal extraction | [111] |
| <i>L. ochroleuca</i> | 39.60 | Extraction with citric acid | This thesis |
| <i>L. ochroleuca</i> | 35.07 | HCl | This thesis |

By analyzing the Table 4, it's possible to conclude that the yield of alginate extracted from *L. ochroleuca* can reach high values, but it is necessary to consider that these values are reached in the most environmentally damaging methods, namely those that use formaldehyde and HCl in the extraction. Considering the greener extraction methods, it's possible to observe that the yields obtained with the optimized protocol (Process 3) is much higher than the ones obtained for example by Flórez-Fernandez *et al.* [110], [111]. Furthermore, comparing the extraction with HCl and citric acid, the yield is slightly higher with citric acid (39.60 %), which is a great advantage for this process, since one of the goals was to achieve a greener method.

Alginate is conventionally isolated using acidic and alkaline solutions to convert its insoluble form in the seaweed cell walls to soluble form (SA). Isolation of alginate using the conventional methods has several disadvantages, such as high energy demand (high temperature), long isolation time and the use of harmful chemicals [112]. With higher temperatures and times, it's possible to obtain a higher yield of alginate, but from an industrial point of view and in order to preserve alginate molecular weight, it is recommended to reduce extraction temperature, usually at room values (25 °C), and extraction time to few hours [61]. With this method, it was possible to reduce the extraction temperatures of conventional methods by maintaining ambient temperature at any step and reduce extraction times. Furthermore, it was possible to reduce the environmental toxicity of the conventional processes by using citric acid instead of the most common used acids. Due to its physicochemical characteristics, citric acid is nontoxic to the environment, degrades rapidly both in sewage works and in surface water and soil. Citric acid is of low acute toxicity to fish, and it's a well-known chelating agent for metals, which provide a good ionic exchange to convert alginate to insoluble alginic acid [95],[76]. Based on the available data, citric acid is not considered a substance that presents a risk to the environment, unlike the acids used in conventional methods such as HCl, H₂SO₄ [76].

II. ATR-FTIR analysis

Figure 17 presents the ATR-FTIR spectra of commercial SA, SA extracted with HCl and SA extracted with citric acid from *L. ochroleuca*, using the extraction Process 3.

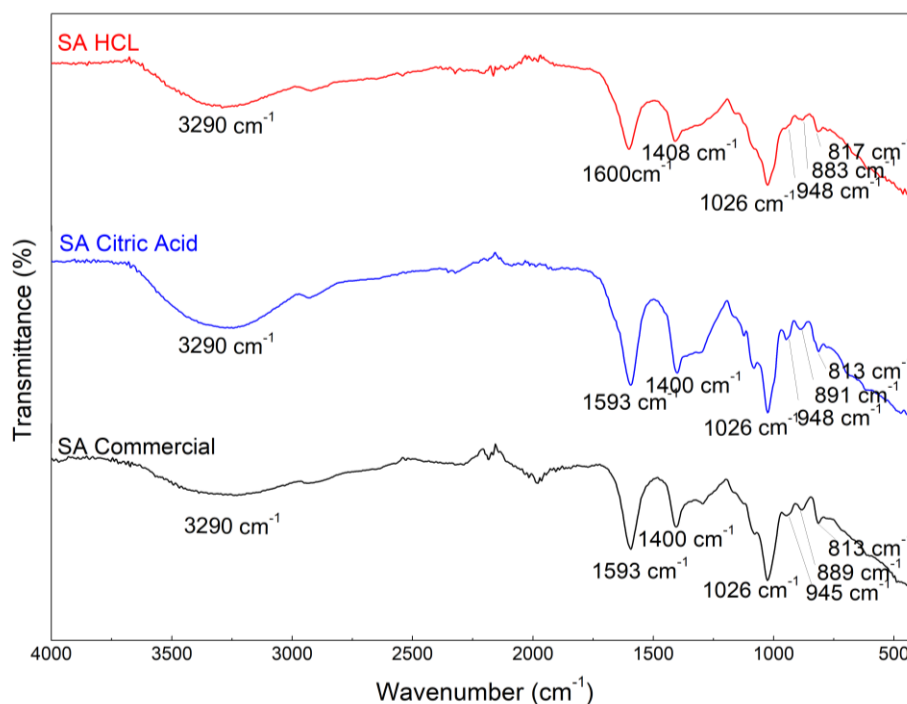


Figure 17 - ATR-FTIR of commercial SA and extracted SA using the Process 3 (with HCl and with citric acid).

The ATR-FTIR spectra of both samples (extraction with HCl and with citric acid), show typical bands of SA, which includes a band at 3290 cm⁻¹, which is attributed to the stretching vibrations of O-H groups, a band at 1593 cm⁻¹ corresponding to carboxylate O-C-O asymmetric stretching vibration and to C=O asymmetric stretching vibrations of uronic acids and peaks at 1400 cm⁻¹ that can be attributed to C-OH deformation vibration and the peak at 1026 cm⁻¹, which is related to C-O and C-C stretching vibrations of pyranoses, with reduced intensity in the extracted samples. SA extracted using the different conditions showed a similar profile with each other and with the commercial SA [58], [93].

III. XRD

In order to analyze the crystallinity of the extracted SA, XRD analysis was performed. The XRD patterns of commercial SA and SA extracted with HCl and citric acid using the extraction Process 3 is represented in Figure 18.

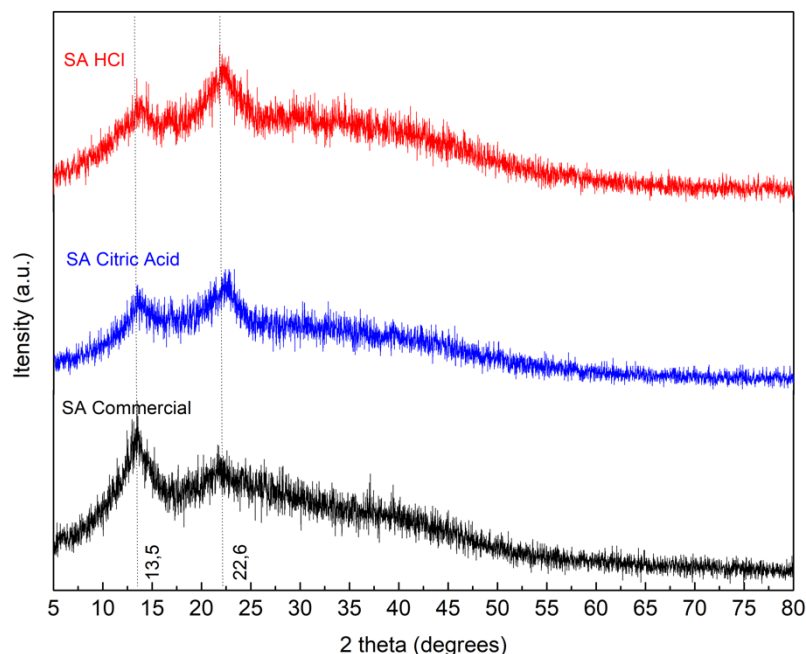


Figure 18 - XRD pattern of commercial SA and extracted SA using Process 3 (with HCl and with citric acid).

The diffraction pattern of commercial SA powder exhibited two different peaks at $2\theta = 13.5^\circ$ and $2\theta = 22.6^\circ$, indicating a semi-crystalline structure. The same XRD pattern was detected for SA extracted with citric acid and HCl, with a crystallinity of 33.98 % and 35.23 %, respectively, calculated using the equation 2 in conjunction with the tool *Origin*, demonstrating its semi-crystalline structure[114]. So, with XRD analysis it can be concluded that both SA extracted from *L. ochroleuca* have similar crystalline structure as commercial SA found in literature, 35.62 %, because the purity of the extracted SA is less than pure SA [114]. There is not a very significant difference in terms of crystallinity of SA using the extraction processes with different acids. So, it can be concluded that the process can be carried out with a weaker and more environmentally friendly acid, citric acid, as intended, without harming the crystalline structure of SA.

$$(2) \quad CI = \frac{\text{Area of all the crystalline peaks}}{\text{Area of all the crystalline and amorphous peaks}}$$

IV. TGA

Finally, the TGA technique was also used to further characterize the sample obtained from the green extraction process, in order to conclude whether the temperatures and degradation intervals coincided with those tabulated for SA in the literature. Figure 19 shows the TGA and DTG spectra obtained for the SA extracted with citric acid, in order to analyze the degradation of the sample.

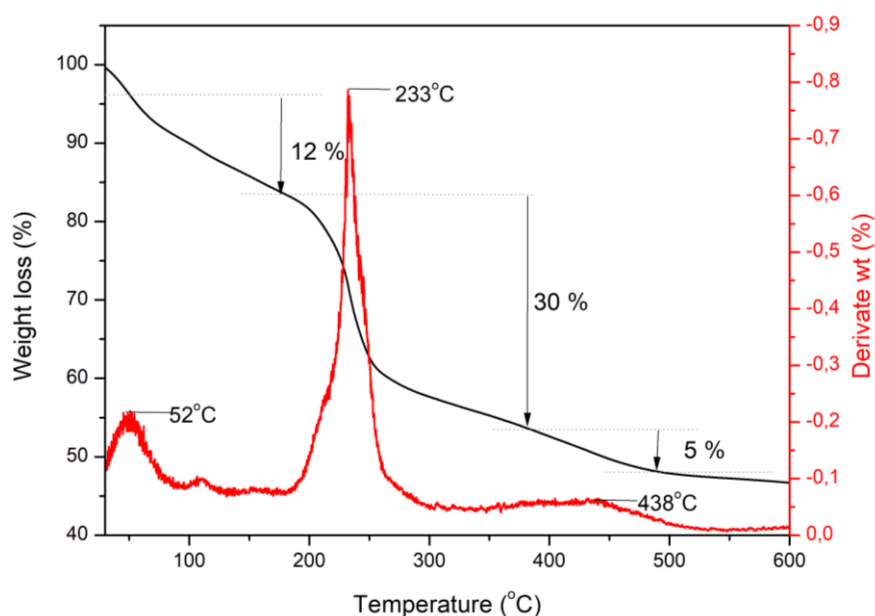


Figure 19 - TGA and DTG curves of SA extracted with the Process 3 using citric acid.

The thermal degradation of extracted SA can be divided into three main mass loss steps. The first one was recorded at 30-180 °C with a mass loss of 12 %, the second stage occurred at 180-370 °C, with a maximum degradation peak at 233 °C, and a weight loss of 30 %, and the third step was detected at 370-500 °C, with a maximum degradation peak at 438 °C, and with a mass loss of 5 %. The TGA of extracted SA agrees with the literature and with other published articles [115]. The weight loss detected in first stage of extracted SA can be attributed to the loss of volatile products like dehydration accompanied by the formation of volatile products. The energy of bonding between water molecules and the sorption sites is higher than the energy that holds the molecules of pure water. The second step is attributed to the depolymerization of polymer associated with the destruction of glycosidic bonds. The third weight loss it could be associated to

the decomposition of the isolated SA, where the fragments and monomeric units of the alginate are converted into Na_2CO_3 [116]. This degradation temperature is close, but slightly higher than degradation temperature of pure SA found in the literature, 200 °C [117].

After the analyses of extraction yield, chemical composition (ATR-FTIR), crystallinity (XRD) and thermal degradation (TGA), it was concluded that SA was successfully extracted using Process 3. Overall, in an environmental perspective, this methodology showed great advantages over the conventional ones, since no temperature and harmful chemicals (e.g., formaldehyde, HCl or H_2SO_4) were used and the extraction time was reduced. Moreover, it allowed to achieve higher extraction yields.

4.2 Nanocellulose extraction

As mentioned earlier, nanocellulose is another polysaccharide that can be extracted from algae, with benefits for electrospun nanofibers to act as wound dressing. The next section shows the results obtained in attempt to extract nanocellulose from *Ulva* spp. algae, using the most green and sustainable process possible. As describe above, *Ulva* spp., converted into powder, was added to a H_2SO_4 solution, and put under reflux, as shown in Figure 10. After that, the hydrolysis was stopped with water, centrifuged and washed with water to reach a pH of 5.5. Finally, the pellet was collected and placed on a dialysis membrane for 6 days. After this procedure, the content of the membrane was poured and dried in the oven at 50 °C. In a second approach, a bleaching pre-treatment was performed, that consisted of placing 4.5 g of algae reduced to powder, in ethanol. Subsequently, the pre-treated algae were washed with ethanol twice and placed in the oven to dry. Then the sample was resuspended with H_2O_2 , and centrifuged, the supernatant was discarded. The pellet was washed with water until it reached pH 7. Afterwards, pellet was added to a solution of NaOH followed by centrifugation and finally placed in the oven at 50 °C. After this pre-treatment, acidic hydrolysis was performed in the same way.

4.2.1. Optical microscopy

An optical microscope was used to analyze the sample extracted from the algae *Ulva* spp. without pre-treatment, in order to see if CNC were present. The images obtained 1 and 6 days after dialysis are shown in Figure 20.

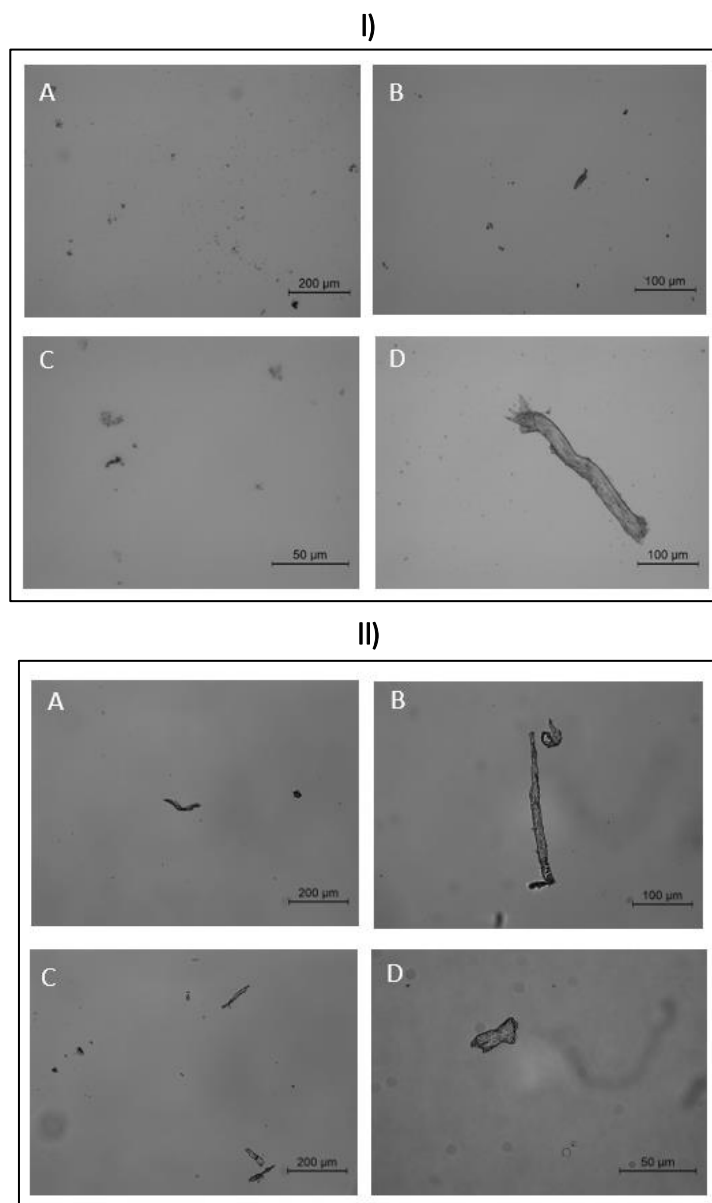


Figure 20 – I) Optical microscopy images of the sample extracted from *Ulva* spp., 1 day after dialysis. **A)** 10x **C)** 50x; **B)** 20x and **D)** 20x; **II)** Optical microscopy images of the sample extracted from *Ulva* spp., 6 days after dialysis. **A)** and **C)** 10x; **B)** 20x; **D)** 50x.

CNCs have crystalline regions (around 54-88 % high crystallinity) and short rod-like shape or whisker shape, with diameter ranging from 2 to 20 nm and length ranging from 100 to 500 nm

[118]. On the images taken the clusters may be nanocellulose crystals but also algae residues, however, many of them are too large to be CNCs. Therefore, STEM analysis would be necessary to verify if there were really CNC in the sample or not. Furthermore, it is also possible to observe, through figures 21I) and 21II), which have different dialysis times, 1 and 6 days, respectively, that the time did not influence the process, and the samples were not reduced, as was supposed.

Based on these findings, a pre-treatment was then developed, as explained above, in order to remove pigments, fatty acids, other colored impurities, the lignin and hemicellulose before the extraction [119], [96]. The obtained sample was analyzed again by optical microscopy (Figure 21).

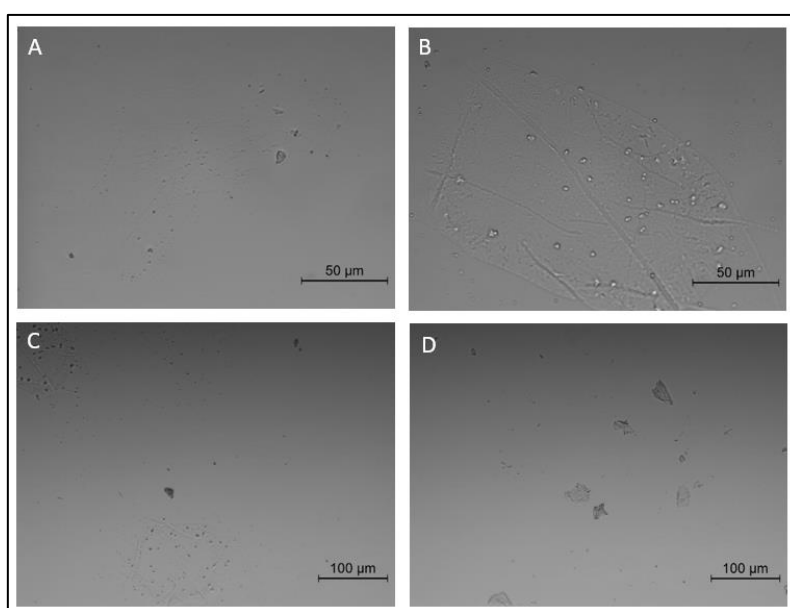


Figure 21 - Optical microscopy images of the sample extracted from *Ulva* spp. with pre-treatment, 6 days after dialysis. **A)** and **B)** 50x; **C)** and **D)** 20x.

By optical microscopy images, it was possible to verify that the sample presented smaller agglomerates in different parts in comparison with the samples without pre-treatment. This can be due to the destruction of the primary fiber cell wall during the removal of the non-cellulosic materials with the pre-treatment [119]. Since it was not possible to verify the needle shape of the CNCs that were expected, by microscopic observation, the extraction was not successful. Among other reasons, this may be due to the fact that the concentration of H_2SO_4 used was too low, since in conventional methods it is used 64 %, or the hydrolysis time was not enough. However, the extraction of SA and the development of electrospun nanofibers with this polymer was prioritized and no further attempts were made for the extraction of nanocellulose from *Ulva* spp..

4.3 Alginate-based electrospun nanofibers

Several solutions with different SA/PVA ratios were developed to design electrospinning membranes for the treatment of skin wounds. In this section, the main results obtained will be discussed. In addition, a natural compound was added to the SA/PVA solutions in order to combat infections associated with skin wounds. Therefore, in this section the main results concerning this will also be presented.

4.3.1. Antibacterial activity of the natural extract

In order to verify the concentration of the natural compound, *Ziziphus*, to be used in the membranes, an antibacterial test was performed as mentioned above. The results, show that of the four concentrations plated (0.625; 0.75; 1.25 and 1.5 mg/mL), there was colony formation of bacteria on the plates whose concentration was 0.625 and 0.75 mg/mL, as shown in Figure 22. On the plates with a concentration of 1.25 and 1.5 mg/mL, no growth of *S. aureus* was recorded, thus the MBC of the natural extract was defined as 1.25 mg/mL.

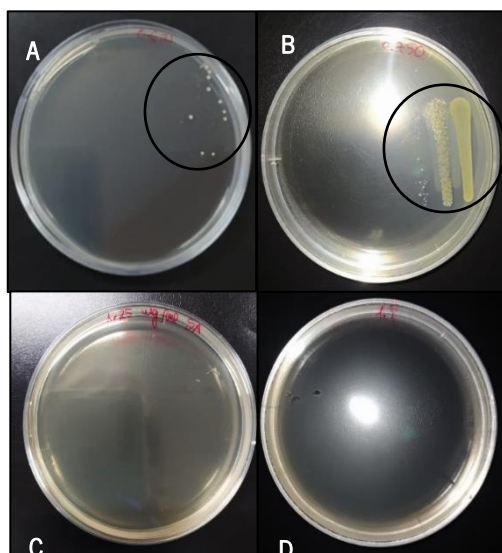


Figure 22 - Plate plates with the different concentrations of *Ziziphus* leaves extract: **(A)** 0.625 mg/mL, **(B)** 0.75 mg/mL, **(C)** 1.25 mg/mL and **(D)** 1.5 mg/mL.

4.3.2. Optimization of the development of alginate-based electrospun nanofibers

As explained before, SA alone constitutes a difficulty for the formation of electrospun nanofibers. Thus, it is necessary to add a polymer, PVA was chosen for all the reasons previously mentioned. So, throughout this work several solutions of SA and PVA as well as their blends (SA/PVA) were evaluated: 2 and 4 % (w/v) SA and 8 and 16 % (w/v) PVA, according to the conditions verified in other articles (Table 5). In addition, several electrospinning parameters were also tested, namely the applied voltage, the distance between the needle and collector and the flow rate, in order to obtain the best condition to produce free-defect nanofibers.

Table 5: Different parameters tested regarding the polymeric solutions and the electrospinning process as well as the main results observed during the process.

| Solution | | Voltage (kV) | Flow rate (mL/h) | Needle-collector distance (cm) | Visual result | | |
|----------------------|----------------------|--------------|------------------------|--------------------------------|--|--------------------|------------------------------|
| Polymeric solution | Ratio | | | | | | |
| SA (2 %)/ PVA (8 %) | 50:50 | 17 | 0.2 | 10 | No jet formation, very liquid solution | | |
| | | 20 | | | | | |
| | 60:40 | 17 | | | | | |
| | | 20 | | | | | |
| SA (2 %)/ PVA (16 %) | 30:70 | 17 | 0.2 | 10 | Light jet | | |
| | | 20-25 | | 10-15 | Droplets | | |
| | | 17 | | 5 | Droplets | | |
| | | 17 | | 10 | Light jet | | |
| | 50:50 | 17 | 0.5 | 10 | Light jet | | |
| | | 24 | | 12 | Deflected jet | | |
| | | 24 | | 12 | 0.5 | Non-continuous jet | |
| | 24 | 0.5 - 1.5 | Non-continuous jet | | | | |
| | SA (4 %)/ PVA (16 %) | 50:50 | 23 | 1 | 12 | Beam with droplets | |
| | | | > 23 | | | | |
| <23 | | | | | | | |
| 24 | | | 7 | | | | Deflected jet |
| 22 | | | 14 | | | | Uniform jet without droplets |
| 60:40 | | 22 | 0.2 | 8 | Light jet with drops | | |
| | | | | 12 | Light jet | | |
| | | | | 14 | Jet | | |
| | | 16 | | Deflected jet | | | |
| | | 17 | | 14 | No jet formation | | |
| | | 26 | | 12 | Jet with droplets | | |
| 70:30 | | 22 | 14 | Jet | | | |
| | | 23 | 10 | Jet with many droplets | | | |
| 80:20 | 22 | 14 | Jet with interruptions | | | | |
| | 17 | 14 | No jet formation | | | | |
| 90:10 | 23 | 0.2 | 10 | Jet with many droplets | | | |
| | 22 | | 14 | Jet with interruptions | | | |
| | 17 | | 14 | No jet formation | | | |

By monitorization of the polymeric jet, it was found that lower flow rates promoted the formation of a more uniform beam, while flow rates higher than 1 led to the formation of droplets. On the other hand, increasing the voltage above 24 kV, a dispersion of the beam was observed and decreasing voltage from 20 kV leads to a jet with drops or not jet et al. Furthermore, it was possible to see that the distance between the needle and the collector also affects the jet and that this is related to the voltage and the flow rate used. However, for very low or very high only droplet deposition or a deflected jet occurs, regardless of the voltage or flow rate used. Thus, after all the trials with the parameters presented in Table 5, it was concluded that the most promising solution was the one with 4 % SA/16 % PVA, since they led to the formation of the most uniform and continuous jet. Therefore, various ratios were then tested with the mentioned SA and PVA concentrations and with the parameters presented in the section Materials and Methods, i.e. with a voltage of 22 kV, a distance between needle and collector of 14 cm, a flow rate of 0.2 mL/h. The experimental ratios are shown in table 6.

Table 6: Electrospun solutions with 4 % SA and 16 % PVA at different ratios.

| INITIAL SOLUTIONS | INITIAL RATIO (SA/PVA) | FINAL CONCENTRATIONS (SA/PVA) |
|---|---------------------------|-------------------------------------|
| SA (4 % (W/V)) + PVA (16 % (W/V)) | 90:10 | 3.6 % / 1.6 % |
| | 80:20 | 3.2 % / 3.2 % |
| | 70:30 | 2.8 % / 4.8 % |
| | 60:40 | 2.4 % / 6.4 % |
| | 50:50 | 2 % / 8 % |

4.3.3. Optical microscopy

In order to evaluate which of the SA/PVA ratios promoted the production of electrospun nanofibers with the best morphology, the optical microscope was used. Figure 23 shows the results obtained for each ratio of the 4 % SA/16 % PVA solution.

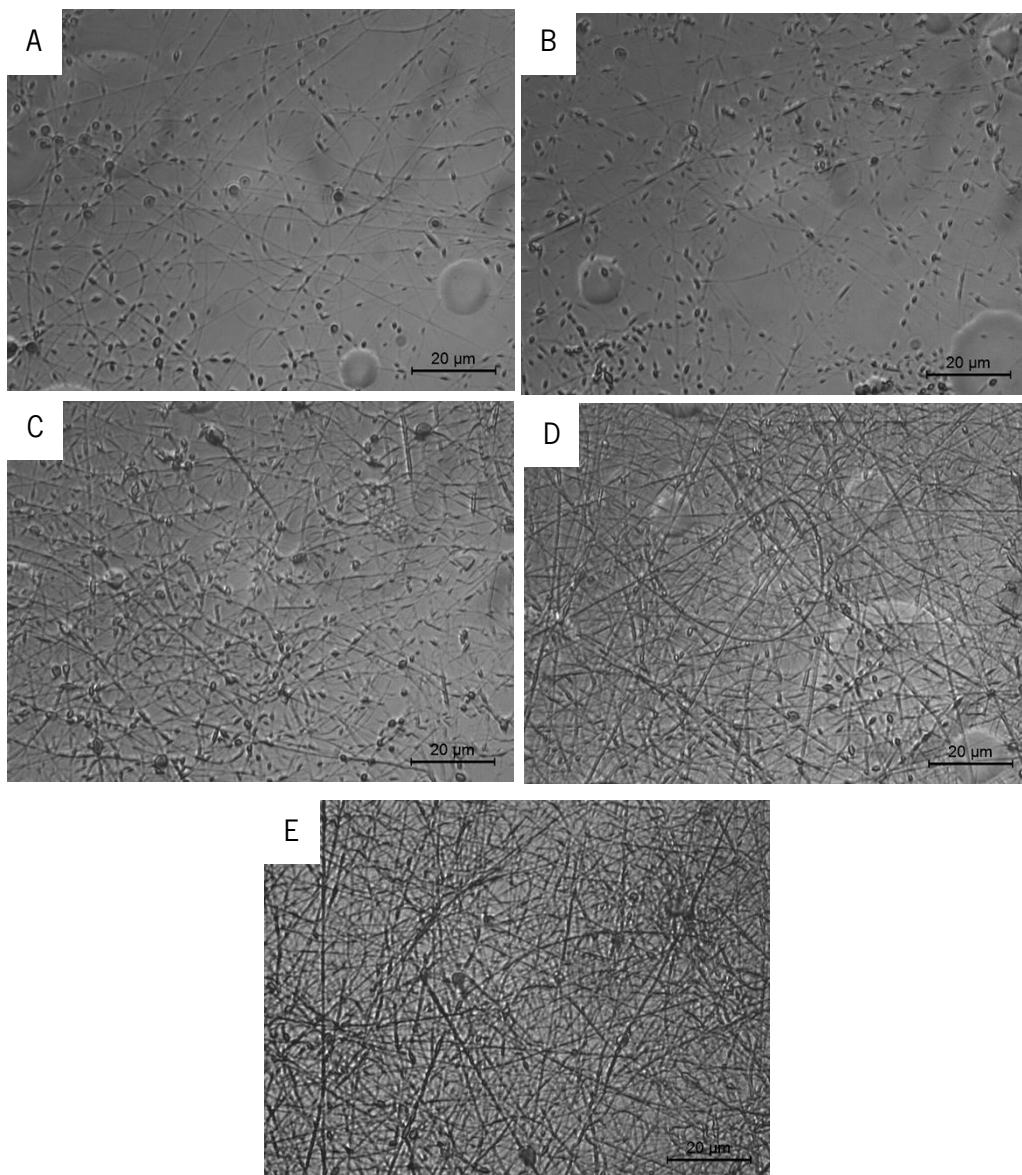


Figure 23 - Microscope images of electrospun SA/PVA nanofibers with different ratios with 100x magnification: **A)** 90:10; **B)** 80:20; **C)** 70:30; **D)** 60:40; **E)** 50:50.

As already explained the addition of another polymer, such as PVA, to the alginate results in better electrospinnability. From Figure 23 it was possible to see that with increasing the percentage of PVA, the better are the morphology of the fibers formed. In fact, the solutions containing higher concentration of SA (SA/PVA: 90:10 and 80:20), only led to the formation of beads. This could be due to high viscosity and surface tension of the solution. Thus, when mixed together with PVA, spinnability is improved due to the hydrogen bonds formed between the two polymers, thereby, the repulsive force between the polyionic molecules is remarkably reduced

to drive chain fusion, which ultimately leads to the production of nanofibers [120]. So, as the concentration of PVA increased, and consequently, the concentration of SA decreased (SA/PVA: 70:30, 60:40 and 50:50), the formation of fibers was visible, as it can be seen in Figure 25 (C, D and E). The increase of PVA concentration, promoted the formation of more continuous fibers with less defects, being the solution of SA/PVA 50:50 the one that presented fibers with improved morphology.

After the analysis by optical microscopy of the various SA/PVA ratios, the membranes were developed with a deposition time of 2 h. The SA/PVA ratios of 90:10, 80:20, 70:30 and 60:40 led to the production of a very thin film, which was impossible to detach from the aluminum foil. On the other hand, it was possible to conclude that the ratio that presented the best results was the 50:50 of the 4 % SA/16 % PVA solution, which presented a visible membrane that was possible to remove from the aluminum foil, but it was also very thin.

4.3.4 Solution viscosity

The characterization of the physical properties of the SA and PVA solution is very important, since the viscosity of the solution is a decisive parameter in the final morphology of the obtained fibers. The viscosity values of the SA, PVA and SA/PVA solution with the optimized ratio are represented in Table 7.

Table 7: Solution viscosity of the polymeric solutions.

| POLYMERIC SOLUTION | VISCOSITY (mPAS) |
|--------------------|------------------|
| SA (4 % w/v) | 40000 |
| PVA (16 % (w/v)) | 17000 |
| SA/PVA (2 % / 8 %) | 2700 |

4.3.5 FESEM

After selecting the solution ratio (SA/PVA 50:50) able to produce the fibers with best morphology, electrospun membranes were produced with 2 h of deposition. Furthermore, the natural extract, *Ziziphus* Leaves, was incorporated into this solution with a final concentration of 1.25 mg/mL (MBC concentration), and an electrospun membrane was also developed using the same electrospinning parameters used to produce SA/PVA membranes. The developed membranes were analyzed by FESEM, as shown in Figure 24.

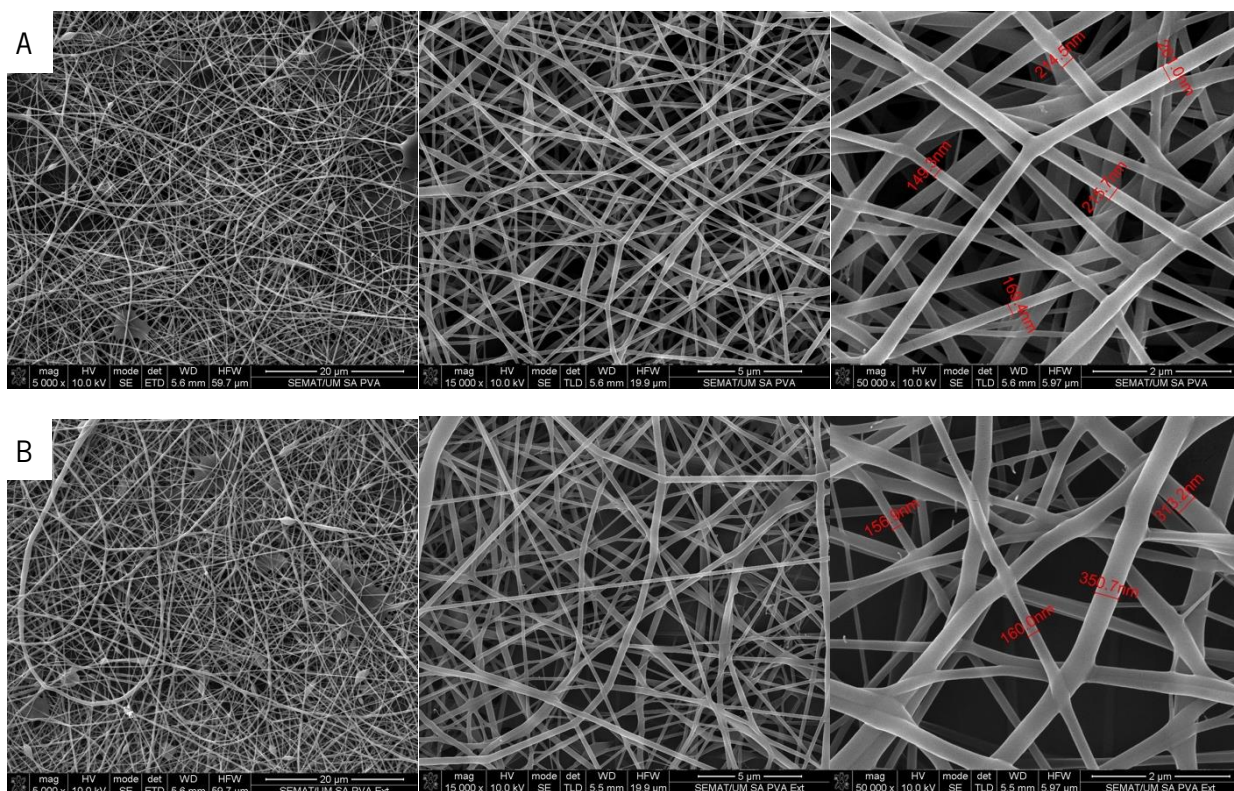


Figure 24 - FESEM images of **A)** SA/PVA and **B)** SA/PVA/ *Ziziphus* electrospun membranes. The FESEM images were obtained using different magnifications, from left to right: 5 000 (20 μm); 15 000x (5 μm); 50 000x (2 μm).

This analysis revealed the presence of uniform fibers with only few beads, confirming the successful development of nanofibers using SA/PVA polymeric formulation. Moreover, the incorporation of the natural extract *Ziziphus* did not affect the morphology of the developed nanofibers, which is advantageous since this antibacterial compound can be incorporated into these membranes without affecting their structure, which is an important parameter for wound dressing. With the help of the ImageJ tool, it was possible to calculate the diameters of the nanofibers in both membranes. The SA/PVA nanofibers showed an average diameter of $170 \pm 54,37$ nm and SA/PVA/ *Ziziphus* nanofibers showed an average diameter of $191 \pm 65,60$ nm, as illustrate in figure 25. The increase in nanofibers' diameters with the addition of the natural extract could be due to the compound entrapment within polymeric chain of nanofibers, leading to large fiber diameter [83].

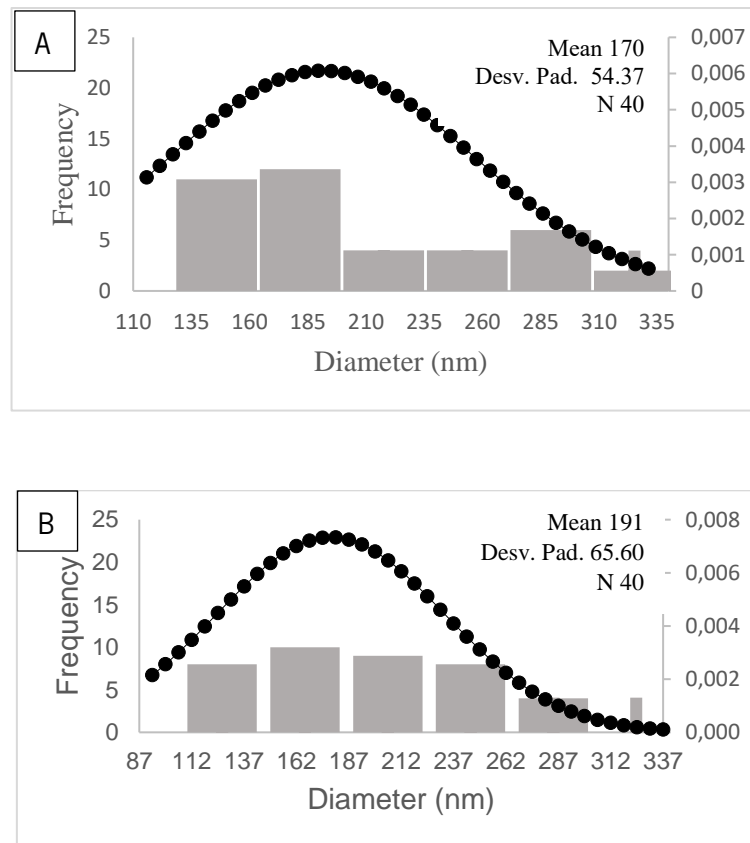


Figure 25 - Diameter distribution histograms of nanofibers: **A)** SA/PVA; **B)** SA/PVA/ *Ziziphus*.

As already said, the electrospinning of individual SA solution is difficult because the gelation of solution starts at very low polymer concentrations (4 wt.%). To solve this problem, it is required to control the sol-gel transition by using incorporating some additives (copolymer or surfactants) which interact with the alginate to reduce the viscosity of solution, so that gelation can occur at a higher polymer concentration [121], [80], in this case PVA. The repulsive force among SA molecules is reduced, and thus electrospinning of PVA/SA blends is successfully allowed from the interaction between PVA and SA. This is due to the intermolecular hydrogen bonding occur between SA and PVA, which resulted in an increase of uniformity and smoothness of the nanofibers. In comparison with the membranes loaded with the natural extract, the diameter is higher as compared to SA/PVA nanofibers, this could be due to the drug entrapped with in polymeric chain of nanofibers leading to large fiber diameter [83].

The objective of this project was to use PVA as a copolymer, i.e., the higher the concentration of SA and the lower the concentration of PVA, the more innovative the work would be and the better it would fit the final application. In this case, it can be state that compared to published studies of nanofibers developed with SA/PVA, it was possible to achieve a promising SA concentration, with a lot of potential, to develop electrospun nanofibers in a uniform way than in most published

studies, which is in line with the goal of this project. Table 8 summarizes the specifications of SA/PVA/*Ziziphus* electrospun nanofibers, with distance between the needle and the collector (D), voltage (V), flow rate (FR) and the needle diameter (Ds).

Table 8: Specifications of SA/PVA/*Ziziphus* electrospun nanofibers

| SA | PVA | Optimal Ratio SA/PVA | Final Concentrations (SA/PVA) | Compound | Electrospinning Parameters | Diameters (nm) | | Ref. |
|-----|------|----------------------|-------------------------------|--|---|----------------|-----------------|-------------|
| | | | | | | SA/PVA | SA/PVA/Compound | |
| 4 % | 16 % | 50:50 | 2 %/8 % | <i>Ziziphus</i> Leaves (Natural Extract) | D = 14 cm V = 22 kV FR = 0.2 mL/h D _n = 0.61 mm | 170 | 191 | This thesis |

4.3.6. ATR-FTIR

In order to analyze the chemical composition of the membranes, as well as the binding of the various compounds, the ATR-FTIR technique was used. Figure 26 shows the ATR-FTIR analysis of the SA/PVA and SA/PVA/*Ziziphus* electrospun membranes.

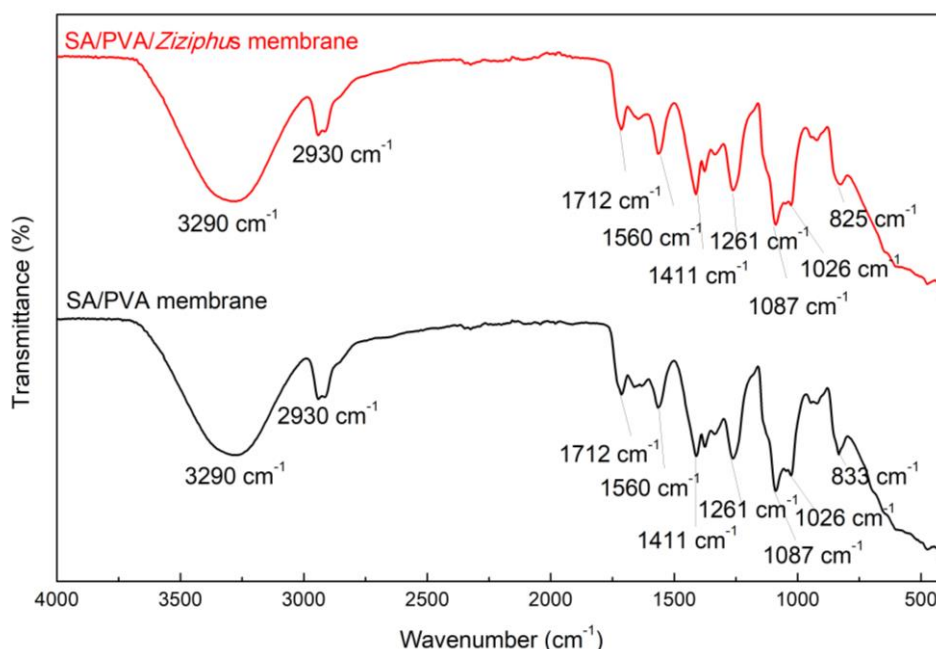


Figure 26 - ATR-FTIR spectra of SA/PVA and SA/PVA/*Ziziphus* electrospun membranes.

ATR-FTIR spectra of the SA/PVA and SA/PVA/*Ziziphus* mats were collected with the purpose of confirming the effectiveness of the polymer blending. SA/PVA spectra contained all the SA and

PVA characteristic bands, yet some peak variations were identified. The ATR-FTIR spectrum of SA/PVA mat, consisted of the following peaks: broad peak at 3290 cm^{-1} , 2930 cm^{-1} , 1712 cm^{-1} , 1560 cm^{-1} that are assigned to the $-\text{OH}$, CH_3 , $-\text{COOH}$, and $\text{C}=\text{C}$ stretching vibration due to the presence of $-\text{COOH}$ and $-\text{OH}$ groups in SA), that indicates the presence of double-bonded functional groups and OH , $\text{C}=\text{C}$ and CH_3 groups in PVA (due to the presence of non-hydrolyzed vinyl acetate groups). These results agree with other published studies [84], [122], [80], [123]. For SA, the characteristic bands appeared at 3290 , 1593 , 1400 , 1026 , 813 , 889 and 945 cm^{-1} and the characteristic bands of PVA at 1725 , 1245 and 840 cm^{-1} [124]. Hydrogen bonding has the strongest influence on the donor and consequently the absorption maxima of stretching vibration shifts toward lower frequencies in comparison with the pure components. This strongly supports the idea that hydrogen bonding could be formed between the oxygen atoms of the hydroxyl groups of PVA and the hydroxyl groups of SA, and even between the PVA chains that remained close together in the blended solution. From this analysis it is possible to verify that the blending of SA and PVA occurred successfully during the electrospinning process [50].

Regarding the SA/PVA/*Ziziphus* membrane, it can be observed that the ATR-FTIR spectrum is very similar to that of the membrane with only SA/PVA, presenting the same band, suggesting that the interaction between the natural extract *Ziziphus* and PVA/SA was not influenced by the electrospinning procedure or due to the equipment low sensitivity for small amounts of the natural extract.

5. CONCLUSIONS AND FUTURE WORK

In recent years, marine macroalgae has received acquiring attention as a very valuable resource of several natural compounds. Therefore, the valorization of this source, frequently presented as waste, for the extraction of biopolymers and bioactive compounds to develop high-value products, including for wound healing application, is of great interest. Thus, this work aimed the extraction of biopolymers, such as alginate and nanocellulose, from different algae, always considering the sustainability of the extraction processes.

A more environmentally friendly method, i.e. without the utilization of toxic solvents, high temperatures and long times, was successfully developed on the *L. ochroleuca* algae. Three attempts of extraction processes were performed, being only the third process proved to be capable of fulfilling the function (Process 3). All the processes carried out were analyzed by various characterization techniques. The first process consisted of an attempted extraction with a mechanical method, using ultrasound combined with citric acid, and follow by Na_2CO_3 for SA precipitation. No precipitate was obtained with this technique, so the sample obtained was analyzed only with UV-Vis, where the absorption waves of the sample (274 nm) have different wavelength than the commercial SA (266 nm). The failure of this process may have been due to the lack of a solvent that precipitates SA, such as ethanol. Thus, this process was discarded and a new one was tested. In Process 2, an initial depigmentation step with ethanol was added, to remove the pigments and algae residues that the previous one did not have, and in addition, ethanol was added to precipitate the SA, ethanol, and then ultrasound was used. A precipitate was obtained and this was characterized as to yield, and the calculated yield was 17.8%, a rather low value compared to several studies; with ATR-FTIR, where it was found very similar bands to pure sodium alginate but some inconsistencies, suggesting that a better washing is needed, so this process was also discarded. Finally, in the last process, there was a depigmentation step, an extraction step, where it was tested with one of the most used but more toxic acids, HCl, and with a weaker acid the citric acid. Afterwards, SA was extracted with Na_2CO_3 , followed by its precipitation with ethanol, and a washing stage with ethanol and acetone. The entire extraction process was performed at room temperature and with reduced times. The samples were analyzed in terms of extraction yield (approximately 40 %), which is in agreement with other developed studies of alginate extraction with green processes; ATR-FTIR, where the characteristic bands of SA were detected; XRD, where the crystalline pattern was very similar to commercial SA, confirming the semi-crystalline structure of the extracted SA and, finally, with TGA, where it was observed the degradation temperature of the extracted SA (180-280°C, with maximum degradation peak at 233 °C), which also goes in

agreement with published data. Thus, with the various analyses it is concluded that SA was successfully extracted from the *L. ochroleuca* algae with an environmentally friendly process. Regarding the extraction process of nanocellulose, it can be said that it was not successfully performed, and therefore, nanocellulose was not used for the development of electrospinning membranes as proposed. Thus, it remains as a proposal for future work.

In the second part of this work, nanofibers were developed by electrospinning with SA extracted from *L. ochroleuca* algae. It was necessary to add a copolymer to allow the electrospinnability of SA. In this case PVA was used, because of its properties, such as biocompatibility and hydrophilicity, which are important for the final application, wound dressings. Thus, two aqueous solutions were prepared, SA (4 % (w/v)) and PVA (16 % (w/v)), and mixed in different ratios of SA/PVA: 50:50; 60:40; 70:30; 80:20; 90:10. All solutions were tested in electrospinning and the produced fibers were analyzed with optical microscopy, which revealed that the SA/PVA ratio 50:50, i.e. with 2 % SA and 8 % PVA, led to the formation of an uniform jet, resulting in the production of nanofibers with average diameters of 170 nm. This concentration of SA was higher than the most already developed, so this was an important point of the work, since the goal was to make wound dressings with as much alginate as possible due to its beneficial characteristics for that application.

Subsequently, a natural extract, *Ziziphus*, was added to the SA/PVA solution (50:50), with a concentration proven to kill *S. aureus*, 1.25 mg/mL. The electrospun membrane was developed with the same electrospinning parameters as the previous ones. Both membranes were analyzed with FESEM and ATR-FTIR techniques. The incorporation of *Ziziphus* extract resulted in uniform nanofibers with diameters of 191 nm, confirming that the addition of the natural extract, as antibacterial agent, did not change the structure of the SA/PVA membranes, which is very important for wound dressing applications. Although the antibacterial activity of the *Ziziphus* extract was tested against *S. aureus*, it was not possible to evaluate the antibacterial activity of the developed membranes to be used in the desired application. Also, other several tests using electrospun membranes should be performed in order to verify their suitability for the final application, such as biocompatibility, absorption capacity, hydrophobicity, drug delivery profile and cytotoxicity. Thus, it is proposed as future work to perform these tests proving that the developed membranes by electrospinning with alginate extracted from algae can be used as bioactive dressings for skin treatments.

6. REFERENCES

- [1] L. Youssouf *et al.*, "Ultrasound-assisted extraction and structural characterization by NMR of alginates and carrageenans from seaweeds," *Carbohydr Polym*, vol. 166, pp. 55–63, Jun. 2017, doi: 10.1016/j.carbpol.2017.01.041.
- [2] M. Gruppuso, G. Turco, E. Marsich, and D. Porrelli, "Polymeric wound dressings, an insight into polysaccharide-based electrospun membranes," *Appl Mater Today*, vol. 24, Sep. 2021, doi: 10.1016/j.apmt.2021.101148.
- [3] A. S. Ribeiro *et al.*, "Chitosan/nanocellulose electrospun fibers with enhanced antibacterial and antifungal activity for wound dressing applications," *React Funct Polym*, vol. 159, Feb. 2021, doi: 10.1016/j.reactfunctpolym.2020.104808.
- [4] S. M. Hosseini, M. Abdouss, S. Mazinani, A. Soltanabadi, and M. Kalae, "Modified nanofiber containing chitosan and graphene oxide-magnetite nanoparticles as effective materials for smart wound dressing," *Compos B Eng*, vol. 231, p. 109557, Feb. 2022, doi: 10.1016/j.compositesb.2021.109557.
- [5] M. Naseri-Nosar and Z. M. Ziora, "Wound dressings from naturally-occurring polymers: A review on homopolysaccharide-based composites," *Carbohydrate Polymers*, vol. 189. Elsevier Ltd, pp. 379–398, Jun. 01, 2018. doi: 10.1016/j.carbpol.2018.02.003.
- [6] P. P. Patil, M. R. Reagan, and R. A. Bohara, "Silk fibroin and silk-based biomaterial derivatives for ideal wound dressings," *International Journal of Biological Macromolecules*, vol. 164. Elsevier B.V., pp. 4613–4627, Dec. 01, 2020. doi: 10.1016/j.ijbiomac.2020.08.041.
- [7] E. M. Tottoli, R. Dorati, I. Genta, E. Chiesa, S. Pisani, and B. Conti, "Skin wound healing process and new emerging technologies for skin wound care and regeneration," *Pharmaceutics*, vol. 12, no. 8. MDPI AG, pp. 1–30, Aug. 01, 2020. doi: 10.3390/pharmaceutics12080735.
- [8] M. A. Teixeira, M. C. Paiva, M. T. P. Amorim, and H. P. Felgueiras, "Electrospun nanocomposites containing cellulose and its derivatives modified with specialized biomolecules for an enhanced wound healing," *Nanomaterials*, vol. 10, no. 3. MDPI AG, Mar. 01, 2020. doi: 10.3390/nano10030557.
- [9] A. S. Ribeiro *et al.*, "Chitosan/nanocellulose electrospun fibers with enhanced antibacterial and antifungal activity for wound dressing applications," *React Funct Polym*, vol. 159, Feb. 2021, doi: 10.1016/j.reactfunctpolym.2020.104808.
- [10] S. Homaeigohar and A. R. Boccaccini, "Antibacterial biohybrid nanofibers for wound dressings," *Acta Biomaterialia*, vol. 107. Acta Materialia Inc, pp. 25–49, Apr. 15, 2020. doi: 10.1016/j.actbio.2020.02.022.
- [11] P. I. Morgado *et al.*, "Poly(vinyl alcohol)/chitosan asymmetrical membranes: Highly controlled morphology toward the ideal wound dressing," *J Memb Sci*, vol. 469, pp. 262–271, Nov. 2014, doi: 10.1016/j.memsci.2014.06.035.

- [12] S. Alven, S. Peter, Z. Mbese, and B. A. Aderibigbe, "Polymer-Based Wound Dressing Materials Loaded with Bioactive Agents: Potential Materials for the Treatment of Diabetic Wounds," *Polymers*, vol. 14, no. 4. MDPI, Feb. 01, 2022. doi: 10.3390/polym14040724.
- [13] L. Tamayo *et al.*, "Coaxial fibers of poly(styrene-co-maleic anhydride)@poly(vinyl alcohol) for wound dressing applications: Dual and sustained delivery of bioactive agents promoting fibroblast proliferation with reduced cell adherence," *Int J Pharm*, vol. 611, Jan. 2022, doi: 10.1016/j.ijpharm.2021.121292.
- [14] S. Homaeigohar and A. R. Boccaccini, "Antibacterial biohybrid nanofibers for wound dressings," *Acta Biomaterialia*, vol. 107. Acta Materialia Inc, pp. 25–49, Apr. 15, 2020. doi: 10.1016/j.actbio.2020.02.022.
- [15] R. S. Ambekar and B. Kandasubramanian, "Advancements in nanofibers for wound dressing: A review," *European Polymer Journal*, vol. 117. Elsevier Ltd, pp. 304–336, Aug. 01, 2019. doi: 10.1016/j.eurpolymj.2019.05.020.
- [16] J. S. Chin, L. Madden, S. Y. Chew, and D. L. Becker, "Drug therapies and delivery mechanisms to treat perturbed skin wound healing," *Advanced Drug Delivery Reviews*, vol. 149–150. Elsevier B.V., pp. 2–18, Sep. 01, 2019. doi: 10.1016/j.addr.2019.03.006.
- [17] M. Gruppuso, G. Turco, E. Marsich, and D. Porrelli, "Polymeric wound dressings, an insight into polysaccharide-based electrospun membranes," *Applied Materials Today*, vol. 24. Elsevier Ltd, Sep. 01, 2021. doi: 10.1016/j.apmt.2021.101148.
- [18] B. Azimi *et al.*, "Bio-based electrospun fibers for wound healing," *Journal of Functional Biomaterials*, vol. 11, no. 3. MDPI AG, Sep. 22, 2020. doi: 10.3390/JFB11030067.
- [19] A. Barbu, B. Neamtu, M. Zăhan, G. M. Iancu, C. Bacila, and V. Mireșan, "Current trends in advanced alginate-based wound dressings for chronic wounds," *Journal of Personalized Medicine*, vol. 11, no. 9. MDPI, Sep. 01, 2021. doi: 10.3390/jpm11090890.
- [20] A. T. Iacob *et al.*, "An overview of biopolymeric electrospun nanofibers based on polysaccharides for wound healing management," *Pharmaceutics*, vol. 12, no. 10. MDPI AG, pp. 1–49, Oct. 01, 2020. doi: 10.3390/pharmaceutics12100983.
- [21] P. I. Morgado *et al.*, "Poly(vinyl alcohol)/chitosan asymmetrical membranes: Highly controlled morphology toward the ideal wound dressing," *J Memb Sci*, vol. 469, pp. 262–271, Nov. 2014, doi: 10.1016/j.memsci.2014.06.035.
- [22] T. A. Kuznetsova, B. G. Andryukov, N. N. Besednova, T. S. Zaporozhets, and A. v. Kalinin, "Marine algae polysaccharides as basis for wound dressings, drug delivery, and tissue engineering: A review," *Journal of Marine Science and Engineering*, vol. 8, no. 7. MDPI AG, Jul. 01, 2020. doi: 10.3390/JMSE8070481.
- [23] S. Wang *et al.*, "Electrospinning of biocompatible alginate-based nanofiber membranes via tailoring chain flexibility," *Carbohydr Polym*, vol. 230, Feb. 2020, doi: 10.1016/j.carbpol.2019.115665.

- [24] D. Shu *et al.*, “One-step electrospinning cellulose nanofibers with superhydrophilicity and superoleophobicity underwater for high-efficiency oil-water separation,” *Int J Biol Macromol*, vol. 162, pp. 1536–1545, Nov. 2020, doi: 10.1016/j.ijbiomac.2020.07.175.
- [25] Y. Liu, M. Park, H. K. Shin, B. Pant, S. J. Park, and H. Y. Kim, “Preparation and characterization of chitosan-based nanofibers by ecofriendly electrospinning,” *Mater Lett*, vol. 132, pp. 23–26, Oct. 2014, doi: 10.1016/j.matlet.2014.06.041.
- [26] S. Ebrahimi, M. Fathi, and M. Kadivar, “Production and characterization of chitosan-gelatin nanofibers by nozzle-less electrospinning and their application to enhance edible film’s properties,” *Food Packag Shelf Life*, vol. 22, Dec. 2019, doi: 10.1016/j.fpsl.2019.100387.
- [27] K. C. Castro, M. G. N. Campos, and L. H. I. Mei, “Hyaluronic acid electrospinning: Challenges, applications in wound dressings and new perspectives,” *International Journal of Biological Macromolecules*, vol. 173. Elsevier B.V., pp. 251–266, Mar. 15, 2021. doi: 10.1016/j.ijbiomac.2021.01.100.
- [28] S. S. Ashraf, K. Parivar, N. Hayati Roodbari, S. Mashayekhan, and N. Amini, “Fabrication and characterization of biaxially electrospun collagen/alginate nanofibers, improved with *Rhodotorula mucilaginosa* sp. GUMS16 produced exopolysaccharides for wound healing applications,” *Int J Biol Macromol*, vol. 196, pp. 194–203, Jan. 2022, doi: 10.1016/j.ijbiomac.2021.11.132.
- [29] F. A. Vieira and S. P. M. Ventura, “Efficient Extraction of Carotenoids from *Sargassum muticum* Using Aqueous Solutions of Tween 20,” *Mar Drugs*, vol. 17, no. 5, May 2019, doi: 10.3390/md17050310.
- [30] A. G. Pereira *et al.*, “The use of invasive algae species as a source of secondary metabolites and biological activities: Spain as case-study,” *Marine Drugs*, vol. 19, no. 4. MDPI AG, Apr. 01, 2021. doi: 10.3390/md19040178.
- [31] A. G. Pereira *et al.*, “The use of invasive algae species as a source of secondary metabolites and biological activities: Spain as case-study,” *Marine Drugs*, vol. 19, no. 4. MDPI AG, Apr. 01, 2021. doi: 10.3390/md19040178.
- [32] P. Q. Nguyen, X. Huang, D. S. Collins, J. J. Collins, and T. Lu, “Harnessing synthetic biology to enhance ocean health,” *Trends in Biotechnology*. Elsevier Ltd, 2023. doi: 10.1016/j.tibtech.2022.12.015.
- [33] S. Khan, M. Naushad, J. Iqbal, C. Bathula, and G. Sharma, “Production and harvesting of microalgae and an efficient operational approach to biofuel production for a sustainable environment,” *Fuel*, vol. 311, p. 122543, Mar. 2022, doi: 10.1016/j.fuel.2021.122543.
- [34] P. S. L. Oscar Serrano Jeffrey J.Kelleway Catherine Lovelock, “Conservation of Blue Carbon Ecosystems for Climate Change Mitigation and Adaptation,” in *Coastal Wetlands (Second Edition)*, 2^a.
- [35] H. M. D. Wang, X. C. Li, D. J. Lee, and J. S. Chang, “Potential biomedical applications of marine algae,” *Bioresource Technology*, vol. 244. Elsevier Ltd, pp. 1407–1415, 2017. doi: 10.1016/j.biortech.2017.05.198.

- [36] P. Otero *et al.*, "Seaweed polysaccharides: Emerging extraction technologies, chemical modifications and bioactive properties," *Critical Reviews in Food Science and Nutrition*. Taylor and Francis Ltd., 2021. doi: 10.1080/10408398.2021.1969534.
- [37] S. Yu, J. Sun, Y. Shi, Q. Wang, J. Wu, and J. Liu, "Nanocellulose from various biomass wastes: Its preparation and potential usages towards the high value-added products," *Environmental Science and Ecotechnology*, vol. 5. Elsevier B.V., Jan. 01, 2021. doi: 10.1016/j.ese.2020.100077.
- [38] L. P. Gomez *et al.*, "Innovative processing strategies and technologies to obtain hydrocolloids from macroalgae for food applications," *Carbohydrate Polymers*, vol. 248. Elsevier Ltd, Nov. 15, 2020. doi: 10.1016/j.carbpol.2020.116784.
- [39] B. G. Andryukov *et al.*, "Sulfated polysaccharides from marine algae as a basis of modern biotechnologies for creating wound dressings: Current achievements and future prospects," *Biomedicines*, vol. 8, no. 9. MDPI AG, Sep. 01, 2020. doi: 10.3390/biomedicines8090301.
- [40] R. Ahmad Raus, W. M. F. Wan Nawawi, and R. R. Nasaruddin, "Alginate and alginate composites for biomedical applications," *Asian Journal of Pharmaceutical Sciences*, vol. 16, no. 3. Shenyang Pharmaceutical University, pp. 280–306, May 01, 2021. doi: 10.1016/j.ajps.2020.10.001.
- [41] K. Iliou, S. Kikionis, E. Ioannou, and V. Roussis, "Marine Biopolymers as Bioactive Functional Ingredients of Electrospun Nanofibrous Scaffolds for Biomedical Applications," *Mar Drugs*, vol. 20, no. 5, p. 314, May 2022, doi: 10.3390/md20050314.
- [42] R. H. M. T. K. , M. N. C. L. Ashok Pandey, *Industrial Biorefineries & White Biotechnology*. 2015.
- [43] A. Salisu, M. M. Sanagi, A. Abu Naim, W. A. Wan Ibrahim, and K. J. Abd Karim, "Removal of lead ions from aqueous solutions using sodium alginate-graft-poly(methyl methacrylate) beads," *Desalination Water Treat*, vol. 57, no. 33, pp. 15353–15361, Jul. 2016, doi: 10.1080/19443994.2015.1071685.
- [44] M. A. N. M. Arash Jahandideh, "Biopolymers in textile industries," in *Biopolymers and their Industrial Applications*, 2021.
- [45] M. Jorfi and E. J. Foster, "Recent advances in nanocellulose for biomedical applications," *Journal of Applied Polymer Science*, vol. 132, no. 14. John Wiley and Sons Inc, Apr. 01, 2015. doi: 10.1002/app.41719.
- [46] A. Qiao *et al.*, "Advances in nanocellulose-based materials as adsorbents of heavy metals and dyes," *Carbohydrate Polymers*, vol. 272. Elsevier Ltd, Nov. 15, 2021. doi: 10.1016/j.carbpol.2021.118471.
- [47] H. Seddiqi *et al.*, "Cellulose and its derivatives: towards biomedical applications," *Cellulose*, vol. 28, no. 4. Springer Science and Business Media B.V., pp. 1893–1931, Mar. 01, 2021. doi: 10.1007/s10570-020-03674-w.

- [48] A. Mahamud, *Production of nanocellulose from sustainable algae marine biomass Fiber Reinforced Polymer Nanocomposites View project Sugar Palm Fibre Reinforced Unsaturated Polyester Composites View project*. [Online]. Available: <https://www.researchgate.net/publication/348759618>
- [49] M. El Achaby, Z. Kassab, A. Aboulkas, C. Gaillard, and A. Barakat, "Reuse of red algae waste for the production of cellulose nanocrystals and its application in polymer nanocomposites," *Int J Biol Macromol*, vol. 106, pp. 681–691, Jan. 2018, doi: 10.1016/j.ijbiomac.2017.08.067.
- [50] S. Ling *et al.*, "Biopolymer nanofibrils: Structure, modeling, preparation, and applications," *Progress in Polymer Science*, vol. 85. Elsevier Ltd, pp. 1–56, Oct. 01, 2018. doi: 10.1016/j.progpolymsci.2018.06.004.
- [51] P. Phanthong, P. Reubroycharoen, X. Hao, G. Xu, A. Abudula, and G. Guan, "Nanocellulose: Extraction and application," *Carbon Resources Conversion*, vol. 1, no. 1. KeAi Publishing Communications Ltd., pp. 32–43, Apr. 01, 2018. doi: 10.1016/j.crcon.2018.05.004.
- [52] G. Hernández-Carmona, Y. Freile-Pelegri, and E. Hernández-Garibay, "Conventional and alternative technologies for the extraction of algal polysaccharides," in *Functional Ingredients from Algae for Foods and Nutraceuticals*, Elsevier Ltd., 2013, pp. 475–516. doi: 10.1533/9780857098689.3.475.
- [53] V. G. P. Putra *et al.*, "An ultrasound-based technique for the analytical extraction of phenolic compounds in red algae," *Arabian Journal of Chemistry*, vol. 15, no. 2, p. 103597, Feb. 2022, doi: 10.1016/j.arabjc.2021.103597.
- [54] S. Saji, A. Hebden, P. Goswami, and C. Du, "A Brief Review on the Development of Alginate Extraction Process and Its Sustainability," *Sustainability (Switzerland)*, vol. 14, no. 9. MDPI, May 01, 2022. doi: 10.3390/su14095181.
- [55] R. A. Khajouei *et al.*, "Extraction and characterization of an alginate from the Iranian brown seaweed *Nizimuddinia zanardini*," *Int J Biol Macromol*, vol. 118, pp. 1073–1081, Oct. 2018, doi: 10.1016/j.ijbiomac.2018.06.154.
- [56] M. Fertah, A. Belfkira, E. montassir Dahmane, M. Taourirte, and F. Brouillette, "Extraction and characterization of sodium alginate from Moroccan *Laminaria digitata* brown seaweed," *Arabian Journal of Chemistry*, vol. 10, pp. S3707–S3714, May 2017, doi: 10.1016/j.arabjc.2014.05.003.
- [57] M. P. Silva, I. J. Badruddin, T. Tonon, S. Rahatekar, and L. D. Gomez, "Environmentally benign alginate extraction and fibres spinning from different European Brown algae species," *Int J Biol Macromol*, vol. 226, pp. 434–442, Jan. 2023, doi: 10.1016/j.ijbiomac.2022.11.306.
- [58] N. Flórez-Fernández, H. Domínguez, and M. D. Torres, "A green approach for alginate extraction from *Sargassum muticum* brown seaweed using ultrasound-assisted technique," *Int J Biol Macromol*, vol. 124, pp. 451–459, Mar. 2019, doi: 10.1016/j.ijbiomac.2018.11.232.

- [59] M. A. Fawzy, M. Gomaa, A. F. Hifney, and K. M. Abdel-Gawad, "Optimization of alginate alkaline extraction technology from *Sargassum latifolium* and its potential antioxidant and emulsifying properties," *Carbohydr Polym*, vol. 157, pp. 1903–1912, Feb. 2017, doi: 10.1016/j.carbpol.2016.11.077.
- [60] L. Youssouf *et al.*, "Ultrasound-assisted extraction and structural characterization by NMR of alginates and carrageenans from seaweeds," *Carbohydr Polym*, vol. 166, pp. 55–63, Jun. 2017, doi: 10.1016/j.carbpol.2017.01.041.
- [61] N. Flórez-Fernández, H. Domínguez, and M. D. Torres, "A green approach for alginate extraction from *Sargassum muticum* brown seaweed using ultrasound-assisted technique," *Int J Biol Macromol*, vol. 124, pp. 451–459, Mar. 2019, doi: 10.1016/j.ijbiomac.2018.11.232.
- [62] N. Flórez-Fernández, M. D. Torres, M. J. González-Muñoz, and H. Domínguez, "Recovery of bioactive and gelling extracts from edible brown seaweed *L. ochroleuca* by non-isothermal autohydrolysis," *Food Chem*, vol. 277, pp. 353–361, Mar. 2019, doi: 10.1016/j.foodchem.2018.10.096.
- [63] N. Wahlström *et al.*, "Cellulose from the green macroalgae *Ulva lactuca*: isolation, characterization, optotracing, and production of cellulose nanofibrils," *Cellulose*, vol. 27, no. 7, pp. 3707–3725, May 2020, doi: 10.1007/s10570-020-03029-5.
- [64] A. F. Tarchoun, D. Trache, and T. M. Klapötke, "Microcrystalline cellulose from *Posidonia oceanica* brown algae: Extraction and characterization," *Int J Biol Macromol*, vol. 138, pp. 837–845, Oct. 2019, doi: 10.1016/j.ijbiomac.2019.07.176.
- [65] E. Zanchetta *et al.*, "Algal cellulose, production and potential use in plastics: Challenges and opportunities," *Algal Research*, vol. 56. Elsevier B.V., Jun. 01, 2021. doi: 10.1016/j.algal.2021.102288.
- [66] A. Aswathi Mohan, A. Robert Antony, K. Greeshma, J. H. Yun, R. Ramanan, and H. S. Kim, "Algal biopolymers as sustainable resources for a net-zero carbon bioeconomy," *Bioresour Technol*, vol. 344. Elsevier Ltd, Jan. 01, 2022. doi: 10.1016/j.biortech.2021.126397.
- [67] I. L. Ross, S. Shah, B. Hankamer, and N. Amiralian, "Microalgal nanocellulose – opportunities for a circular bioeconomy," *Trends in Plant Science*, vol. 26, no. 9. Elsevier Ltd, pp. 924–939, Sep. 01, 2021. doi: 10.1016/j.tplants.2021.05.004.
- [68] B. Qu and Y. Luo, "Preparation and characterization of carboxymethyl cellulose capped zinc oxide nanoparticles: A proof-of-concept study," *Food Chem*, vol. 389, Sep. 2022, doi: 10.1016/j.foodchem.2022.133001.
- [69] K. L. Spence, R. A. Venditti, O. J. Rojas, Y. Habibi, and J. J. Pawlak, "A comparative study of energy consumption and physical properties of microfibrillated cellulose produced by different processing methods," *Cellulose*, vol. 18, no. 4, pp. 1097–1111, Aug. 2011, doi: 10.1007/s10570-011-9533-z.

- [70] S. Sankhla, H. H. Sardar, and S. Neogi, "Greener extraction of highly crystalline and thermally stable cellulose micro-fibers from sugarcane bagasse for cellulose nano-fibrils preparation," *Carbohydr Polym*, vol. 251, Jan. 2021, doi: 10.1016/j.carbpol.2020.117030.
- [71] N. Wahlström *et al.*, "Cellulose from the green macroalgae *Ulva lactuca*: isolation, characterization, optotracing, and production of cellulose nanofibrils," *Cellulose*, vol. 27, no. 7, pp. 3707–3725, May 2020, doi: 10.1007/s10570-020-03029-5.
- [72] Y. W. Chen, H. V. Lee, J. C. Juan, and S. M. Phang, "Production of new cellulose nanomaterial from red algae marine biomass *Gelidium elegans*," *Carbohydr Polym*, vol. 151, pp. 1210–1219, Oct. 2016, doi: 10.1016/j.carbpol.2016.06.083.
- [73] A. D. Juncos Bombin, N. J. Dunne, and H. O. McCarthy, "Electrospinning of natural polymers for the production of nanofibres for wound healing applications," *Materials Science and Engineering C*, vol. 114. Elsevier Ltd, Sep. 01, 2020. doi: 10.1016/j.msec.2020.110994.
- [74] L. Z. C. H. X. J. Bilal Zaarour, "A mini review on the generation of crimped ultrathin fibers via electrospinning: Materials, strategies, and applications," 2020.
- [75] S. M. Tan *et al.*, "Electrospinning and its potential in fabricating pharmaceutical dosage form," *Journal of Drug Delivery Science and Technology*, vol. 76. Editions de Sante, Oct. 01, 2022. doi: 10.1016/j.jddst.2022.103761.
- [76] M. Keshvardoostchokami, S. S. Majidi, P. Huo, R. Ramachandran, M. Chen, and B. Liu, "Electrospun nanofibers of natural and synthetic polymers as artificial extracellular matrix for tissue engineering," *Nanomaterials*, vol. 11, no. 1. MDPI AG, pp. 1–23, Jan. 01, 2021. doi: 10.3390/nano11010021.
- [77] S. Fahimirad and F. Ajalloueiian, "Naturally-derived electrospun wound dressings for target delivery of bio-active agents," *International Journal of Pharmaceutics*, vol. 566. Elsevier B.V., pp. 307–328, Jul. 20, 2019. doi: 10.1016/j.ijpharm.2019.05.053.
- [78] P. Ni *et al.*, "Electrospun preparation and biological properties in vitro of polyvinyl alcohol/sodium alginate/nano-hydroxyapatite composite fiber membrane," *Colloids Surf B Biointerfaces*, vol. 173, pp. 171–177, Jan. 2019, doi: 10.1016/j.colsurfb.2018.09.074.
- [79] S. Arthanari *et al.*, "Preparation and characterization of gatifloxacin-loaded alginate/poly (vinyl alcohol) electrospun nanofibers," *Artif Cells Nanomed Biotechnol*, vol. 44, no. 3, pp. 847–852, Apr. 2016, doi: 10.3109/21691401.2014.986676.
- [80] K. T. Shalumon, K. H. Anulekha, S. v. Nair, S. v. Nair, K. P. Chennazhi, and R. Jayakumar, "Sodium alginate/poly(vinyl alcohol)/nano ZnO composite nanofibers for antibacterial wound dressings," *Int J Biol Macromol*, vol. 49, no. 3, pp. 247–254, 2011, doi: 10.1016/j.ijbiomac.2011.04.005.
- [81] E. A. Kamoun, S. A. Loutfy, Y. Hussein, and E. R. S. Kenawy, "Recent advances in PVA-polysaccharide based hydrogels and electrospun nanofibers in biomedical applications: A

- review," *International Journal of Biological Macromolecules*, vol. 187. Elsevier B.V., pp. 755–768, Sep. 30, 2021. doi: 10.1016/j.ijbiomac.2021.08.002.
- [82] R. Fu *et al.*, "A novel electrospun membrane based on moxifloxacin hydrochloride/poly(vinyl alcohol)/sodium alginate for antibacterial wound dressings in practical application," *Drug Deliv*, vol. 23, no. 3, pp. 828–839, Mar. 2016, doi: 10.3109/10717544.2014.918676.
- [83] Y. Tang *et al.*, "Honey loaded alginate/PVA nanofibrous membrane as potential bioactive wound dressing," *Carbohydr Polym*, vol. 219, pp. 113–120, Sep. 2019, doi: 10.1016/j.carbpol.2019.05.004.
- [84] S. Arthanari *et al.*, "Preparation and characterization of gatifloxacin-loaded alginate/poly (vinyl alcohol) electrospun nanofibers," *Artif Cells Nanomed Biotechnol*, vol. 44, no. 3, pp. 847–852, Apr. 2016, doi: 10.3109/21691401.2014.986676.
- [85] K. T. Shalumon, K. H. Anulekha, S. v. Nair, S. v. Nair, K. P. Chennazhi, and R. Jayakumar, "Sodium alginate/poly(vinyl alcohol)/nano ZnO composite nanofibers for antibacterial wound dressings," *Int J Biol Macromol*, vol. 49, no. 3, pp. 247–254, 2011, doi: 10.1016/j.ijbiomac.2011.04.005.
- [86] P. Ni *et al.*, "Electrospun preparation and biological properties in vitro of polyvinyl alcohol/sodium alginate/nano-hydroxyapatite composite fiber membrane," *Colloids Surf B Biointerfaces*, vol. 173, pp. 171–177, Jan. 2019, doi: 10.1016/j.colsurfb.2018.09.074.
- [87] İ. Esentürk, T. Balkan, S. Güngör, S. Saraç, and M. S. Erdal, "Preparation and characterization of naftifine-loaded poly(vinyl alcohol)/sodium alginate electrospun nanofibers," *Brazilian Journal of Pharmaceutical Sciences*, vol. 56, 2020, doi: 10.1590/S2175-97902019000318440.
- [88] M. E. Talukder *et al.*, "Chitosan-functionalized sodium alginate-based electrospun nanofiber membrane for As (III) removal from aqueous solution," *J Environ Chem Eng*, vol. 9, no. 6, Dec. 2021, doi: 10.1016/j.jece.2021.106693.
- [89] T. Krell and M. A. Matilla, "Antimicrobial resistance: progress and challenges in antibiotic discovery and anti-infective therapy," *Microb Biotechnol*, vol. 15, no. 1, pp. 70–78, Jan. 2022, doi: 10.1111/1751-7915.13945.
- [90] K. H. R. E. W. H. Irith Wiegand, "Agar and broth dilution methods to determine the minimal inhibitory concentration (MIC) of antimicrobial substances," *Nat Protoc*, 2008.
- [91] A. I. Hassan and E. I. Abdel-Gawad, "Effect of Zizyphus Leaves Extract on Mice Suffering from Ehrlich Ascites Carcinoma," 2010. [Online]. Available: <http://www.sciencepub.net/nature>
- [92] B. Trica *et al.*, "Extraction and Characterization of Alginate from an Edible Brown Seaweed (*Cystoseira barbata*) Harvested in the Romanian Black Sea," *Mar Drugs*, vol. 17, no. 7, 2019, doi: 10.3390/md17070405.
- [93] M. Fertah, A. Belfkira, E. montassir Dahmane, M. Taourirte, and F. Brouillette, "Extraction and characterization of sodium alginate from Moroccan *Laminaria digitata* brown seaweed,"

- Arabian Journal of Chemistry*, vol. 10, pp. S3707–S3714, May 2017, doi: 10.1016/j.arabjc.2014.05.003.
- [94] M. A. Fawzy and M. Gomaa, "Optimization of citric acid treatment for the sequential extraction of fucoidan and alginate from *Sargassum latifolium* and their potential antioxidant and Fe(III) chelation properties", doi: 10.1007/s10811-021-02453-9/Published.
- [95] M. A. Fawzy, M. Gomaa, A. F. Hifney, and K. M. Abdel-Gawad, "Optimization of alginate alkaline extraction technology from *Sargassum latifolium* and its potential antioxidant and emulsifying properties," *Carbohydr Polym*, vol. 157, pp. 1903–1912, Feb. 2017, doi: 10.1016/j.carbpol.2016.11.077.
- [96] N. Wahlström *et al.*, "Cellulose from the green macroalgae *Ulva lactuca*: isolation, characterization, optotracing, and production of cellulose nanofibrils," *Cellulose*, vol. 27, no. 7, pp. 3707–3725, May 2020, doi: 10.1007/s10570-020-03029-5.
- [97] V. Puca *et al.*, "Microbial species isolated from infected wounds and antimicrobial resistance analysis: Data emerging from a three-years retrospective study," *Antibiotics*, vol. 10, no. 10, Oct. 2021, doi: 10.3390/antibiotics10101162.
- [98] S. H. Rashedy, M. S. M. Abd El Hafez, M. A. Dar, J. Cotas, and L. Pereira, "Evaluation and characterization of alginate extracted from brown seaweed collected in the red sea," *Applied Sciences (Switzerland)*, vol. 11, no. 14, Jul. 2021, doi: 10.3390/app11146290.
- [99] "The Basics of UV-Vis Spectrophotometry A primer."
- [100] T. Petit and L. Puskar, "FTIR spectroscopy of nanodiamonds: Methods and interpretation," *Diamond and Related Materials*, vol. 89. Elsevier Ltd, pp. 52–66, Oct. 01, 2018. doi: 10.1016/j.diamond.2018.08.005.
- [101] Augusto Di Gianfrancesco, "Technologies for chemical analyses, microstructural and inspection investigations," in *Materials for ultra-supercritical and advanced ultra-supercritical power plants*, 2017.
- [102] R. M. D. K. S. R. Y.-O. M. B. C. R. K. T. Nidhi Raval, "Chapter 10 - Importance of Physicochemical Characterization of Nanoparticles in Pharmaceutical Product Development," in *Basic Fundamentals of Drug Delivery*, 2019, pp. 369–400.
- [103] A. H. R. M. M. Q. A. R. R. Amina Sarfraz, "Electrode Materials for Fuel Cells," in *Encyclopedia of Smart Materials*, 2022, pp. 341–356.
- [104] J. Rydz, A. Šišková, and A. Andicsová Eckstein, "Scanning Electron Microscopy and Atomic Force Microscopy: Topographic and Dynamical Surface Studies of Blends, Composites, and Hybrid Functional Materials for Sustainable Future," *Advances in Materials Science and Engineering*, vol. 2019, 2019, doi: 10.1155/2019/6871785.
- [105] A. J. Lorbeer, J. Lahnstein, G. B. Fincher, P. Su, and W. Zhang, "Kinetics of conventional and microwave-assisted fucoidan extractions from the brown alga, *Ecklonia radiata*," *J Appl Phycol*, vol. 27, no. 5, pp. 2079–2087, Oct. 2015, doi: 10.1007/s10811-014-0446-8.

- [106] R. A. Khajouei *et al.*, "Extraction and characterization of an alginate from the Iranian brown seaweed *Nizimuddinia zanardini*," *Int J Biol Macromol*, vol. 118, pp. 1073–1081, Oct. 2018, doi: 10.1016/j.ijbiomac.2018.06.154.
- [107] "Database of ATR-FT-IR spectra of various materials."
- [108] S. Kaidi *et al.*, "Isolation and Structural Characterization of Alginates from the Kelp Species *L. ochroleuca* and *Saccorhiza polyschides* from the Atlantic Coast of Morocco," *Colloids and Interfaces*, vol. 6, no. 4, p. 51, Sep. 2022, doi: 10.3390/colloids6040051.
- [109] Z. Belattmania *et al.*, "Isolation and FTIR-ATR and ¹H NMR characterization of alginates from the main alginophyte species of the atlantic coast of Morocco," *Molecules*, vol. 25, no. 18, Sep. 2020, doi: 10.3390/molecules25184335.
- [110] N. Flórez-Fernández, M. D. Torres, M. J. González-Muñoz, and H. Domínguez, "Recovery of bioactive and gelling extracts from edible brown seaweed *L. ochroleuca* by non-isothermal autohydrolysis," *Food Chem*, vol. 277, pp. 353–361, Mar. 2019, doi: 10.1016/j.foodchem.2018.10.096.
- [111] N. Flórez-Fernández, M. Álvarez-Vinãs, F. Guerreiro, M. D. Torres, A. Grenha, and H. Domínguez, "Hydrothermal Processing of *L. ochroleuca* for the Production of Crude Extracts Used to Formulate Polymeric Nanoparticles," *Mar Drugs*, vol. 18, no. 7, Jul. 2020, doi: 10.3390/md18070336.
- [112] S. Jeddi, M. Rezaei, and M. Alboofetileh, "Impact of green extraction methods on the structural, morphological, physico-mechanical, and thermal properties of alginate films of *Sargassum ilicifolium*," *J Food Process Preserv*, Sep. 2022, doi: 10.1111/jfpp.17081.
- [113] "OECD SIDS CITRIC ACID UNEP PUBLICATIONS 2 SIDS Initial Assessment Report for 11 th SIAM," 2000.
- [114] S. N. Kane, A. Mishra, and A. K. Dutta, "Preface: International Conference on Recent Trends in Physics (ICRTP 2016)," *Journal of Physics: Conference Series*, vol. 755, no. 1. Institute of Physics Publishing, Nov. 01, 2016. doi: 10.1088/1742-6596/755/1/011001.
- [115] A. Salisu, M. M. Sanagi, A. Abu Naim, K. J. Abd Karim, W. A. Wan Ibrahim, and U. Abdulganiyu, "Alginate graft polyacrylonitrile beads for the removal of lead from aqueous solutions," *Polymer Bulletin*, vol. 73, no. 2, pp. 519–537, Feb. 2016, doi: 10.1007/s00289-015-1504-3.
- [116] C. G. Flores-Hernández, M. de los A. Cornejo-Villegas, A. Moreno-Martell, and A. del Real, "Synthesis of a biodegradable polymer of poly (Sodium alginate/ethyl acrylate)," *Polymers (Basel)*, vol. 13, no. 4, pp. 1–12, Feb. 2021, doi: 10.3390/polym13040504.
- [117] S. G. Reddy and A. Thakur, "Thermal stability and kinetics of sodium alginate and lignosulphonic acid blends," *Iranian Journal of Materials Science and Engineering*, vol. 15, no. 3, pp. 53–59, 2018, doi: 10.22068/ijmse.15.3.53.
- [118] C. A. D. S. Mahendra Rai, *Applications in Food Packaging and Wound Healing*. 2021.

- [119] Y. W. Chen, H. V. Lee, J. C. Juan, and S. M. Phang, "Production of new cellulose nanomaterial from red algae marine biomass *Gelidium elegans*," *Carbohydr Polym*, vol. 151, pp. 1210–1219, Oct. 2016, doi: 10.1016/j.carbpol.2016.06.083.
- [120] S. Jadbabaei, M. Kolahdoozan, F. Naeimi, and H. Ebadi-Dehaghani, "Preparation and characterization of sodium alginate-PVA polymeric scaffolds by electrospinning method for skin tissue engineering applications," *RSC Adv*, vol. 11, no. 49, pp. 30674–30688, Aug. 2021, doi: 10.1039/d1ra04176b.
- [121] K. Kataria, A. Gupta, G. Rath, R. B. Mathur, and S. R. Dhakate, "In vivo wound healing performance of drug loaded electrospun composite nanofibers transdermal patch," *Int J Pharm*, vol. 469, no. 1, pp. 102–110, Jul. 2014, doi: 10.1016/j.ijpharm.2014.04.047.
- [122] R. Fu *et al.*, "A novel electrospun membrane based on moxifloxacin hydrochloride/poly(vinyl alcohol)/sodium alginate for antibacterial wound dressings in practical application," *Drug Deliv*, vol. 23, no. 3, pp. 828–839, Mar. 2016, doi: 10.3109/10717544.2014.918676.
- [123] M. E. Talukder *et al.*, "Chitosan-functionalized sodium alginate-based electrospun nanofiber membrane for As (III) removal from aqueous solution," *J Environ Chem Eng*, vol. 9, no. 6, Dec. 2021, doi: 10.1016/j.jece.2021.106693.
- [124] M. A. Teixeira *et al.*, "Antibacterial and hemostatic capacities of cellulose nanocrystalline-reinforced poly(vinyl alcohol) electrospun mats doped with Tiger 17 and pexiganan peptides for prospective wound healing applications," *Biomaterials Advances*, vol. 137, Jun. 2022, doi: 10.1016/j.bioadv.2022.212830.